Biogeosciences Discuss., 12, 12975–13039, 2015
www.biogeosciences-discuss.net/12/12975/2015/
doi:10.5194/bgd-12-12975-2015

Biogeosciences Discussions
Open Access

Improved end-member characterization of modern organic matter pools in the Ohrid Basin (Albania, Macedonia) and evaluation of new palaeoenvironmental proxies

J. Holtvoeth[1,2], D. Rushworth[1], A. Imeri[3], M. Cara[3], H. Vogel[4], T. Wagner[5], and G. A. Wolff[1]

[1]Department of Earth, Ocean and Ecological Sciences, School of Environmental Sciences, University of Liverpool, Liverpool, UK
[2]School of Chemistry, Organic Geochemistry Unit, University of Bristol, Bristol, UK
[3]Faculty of Agriculture and Environment, Agricultural University of Tirana, Tirana, Albania
[4]Institute of Geological Sciences & Oeschger Centre for Climate Change Research, University of Bern, Bern, Switzerland
[5]School of Civil Engineering & Geosciences, University of Newcastle, Newcastle-upon-Tyne, UK

Received: 25 June 2015 – Accepted: 3 July 2015 – Published: 13 August 2015

Correspondence to: J. Holtvoeth (j.holtvoeth@bristol.ac.uk)

Published by Copernicus Publications on behalf of the European Geosciences Union.

BGD
12, 12975–13039, 2015

Abstract

We present elemental, lipid biomarker and compound-specific isotope ($\delta^{13}C$, $\delta^{2}H$) data for soils and leaf litter collected in the catchment of Lake Ohrid (Albania, Macedonia), as well as macrophytes, particulate organic matter and sediments from the lake itself. Lake Ohrid provides an outstanding archive of continental environmental change of at least 1.2 M years and the purpose of our study is to ground truth organic geochemical proxies that we developed in order to study past changes in the terrestrial biome. We show that soils dominate the lipid signal of the lake sediments rather than the vegetation or aquatic biomass, while compound-specific isotopes ($\delta^{13}C$, $\delta^{2}H$) determined for *n*-alkanoic acids confirm a dominant terrestrial source of organic matter to the lake. There is a strong imprint of suberin monomers on the composition of total lipid extracts and chain-length distributions of *n*-alkanoic acids, *n*-alcohols, *ω*-hydroxy acids and *α*,*ω*-dicarboxylic acids. Our end-member survey identifies that ratios of mid-chain length suberin-derived to long-chain length cuticular-derived alkyl compounds as well as their average chain length distributions can be used as new molecular proxies of organic matter sources to the lake. We tested these for the 8.2 ka event, a pronounced and widespread Holocene climate fluctuation. In SE Europe climate became drier and cooler in response to the event, as is clearly recognizable in the carbonate and organic carbon records of Lake Ohrid sediments. Our new proxies indicate biome modification in response to hydrological changes, identifying two phases of increased soil OM supply, first from topsoils and then from mineral soils. Our study demonstrates that geochemical fingerprinting of terrestrial OM should focus on the main lipid sources, rather than the living biomass. Both can exhibit climate-controlled variability, but are generally not identical.

BGD
12, 12975–13039, 2015

1 Introduction

Climate-controlled changes in hydrology are reflected in the development of the terrestrial biome, which determines the amount and the quality of organic matter (OM) supplied to environmental archives (Meyers and Lallier-Vergès, 1999). Currently, reconstructions of biome dynamics are largely based on pollen data, focussing on the development of the vegetation (Birks and Birks, 2006). The dynamics of the soil organic carbon pool, however, is poorly constrained, mainly because palynologists cannot easily discriminate between direct supply of pollen and intermediate storage of pollen in soils. Similarly, paleoclimatologists using established organic geochemical proxies such as the organic carbon to nitrogen ratio (C/N) or bulk organic carbon isotopes ($\delta^{13}C_{org}$) to identify changing proportions of OM from aquatic and terrestrial sources struggle to differentiate between the individual elements of the terrigenous OM pool. Particularly problematic is the variable composition of terrestrial OM resulting from changing proportions of soil and plant litter and the degree of biological degradation that is closely related to the moisture regime. Furthermore, potential end-member materials are often not properly defined and proxies are transferred between supposedly comparable settings untested, reducing their actual applicability and potentially leading to erroneous interpretations.

We focus on Lake Ohrid in the Western Balkans (Fig. 1), which provides an outstanding archive of continental environmental change dating back at least 1.2 M years (Wagner et al., 2014). In 2013, almost 600 m of sediment core was recovered during a drilling campaign for the International Continental Drilling Program (ICDP). Initial analyses of core catcher material and logging data reveal a continuous limnic sequence, showing pronounced cyclicity that clearly relates to eccentricity and obliquity cycles (Wagner et al., 2014; B. Wagner, T. Wonik, personal communication, 2014). This exceptional continental sediment record thus appears very promising for high-resolution palaeoenvironmental reconstructions of orbitally controlled Northern Hemisphere climate fluctuations. Earlier studies of pilot cores suggest a close relationship between the North

BGD
12, 12975–13039, 2015

Atlantic climate of the past 130 000 years and the sedimentation of inorganic as well as organic matter in the lake (Vogel et al., 2010; Holtvoeth et al., 2010). Whichever proxy is used to reconstruct changes in biogeochemical fluxes towards a sedimentary archive, the sources of each component have to be known in order to correctly interpret proxy variability. For distal marine sediment archives, mixing associated with long-distance transport results in averaged end-member characteristics for marine and terrestrially-sourced matter that are reasonably well defined. Terrestrial ecosystems, by contrast, show far greater complexity and diversity, with a great variety of local factors and processes that modify specific end-members. The local vegetation type, geology, geomorphology or hydrology may all reveal peculiarities that potentially interfere with the regional or global climate signal that paleoclimatologists are keen to extract from terrestrial archives.

As part of a longer term study of the Ohrid sedimentary record, we aim to improve the end-member definition of organic matter (OM) sources, and test new geochemical proxies across the 8.2 ka climate event. We provide lipid biomarker distributions, compound-specific carbon and hydrogen stable isotopic ($\delta^{13}C$, $\delta^{2}H$) and elemental compositions of modern materials from the Lake Ohrid Basin, including terrestrial plant litter, soils, macrophytes and lake water filtrates, all of which may influence the geochemical signature of the OM deposited in the lake.

A great advantage of the Lake Ohrid climate archive is its small, mountainous catchment (Fig. 1). Up to 55 % of water inflow derives from karst springs fed by seepage from the higher altitude Lake Prespa. Although these waters do not deliver any sediment they do supply small amounts of nutrients to Lake Ohrid, e.g., 7 % of the total phosphorous load (Matzinger et al., 2006), as well as calcium ions allowing carbonate precipitation. As there are no major rivers entering the Ohrid Basin, the supply of allochthonous sediment to the lake depends almost entirely on surface run-off from the surrounding mountain ranges in the form of small streams and gullies. The Triassic limestones forming the eastern, southeastern and northwestern slopes of the Ohrid Basin are highly permeable so that much of the precipitation is taken up by karstic

BGD
12, 12975–13039, 2015

systems before reaching the lake. Thus, the quantity and composition of terrestrial OM supplied to the lake will reflect hydrologically-controlled changes in vegetation and soil stocks of the immediate surroundings, while productivity in the lake reflects run-off-controlled nutrient supply. The steep morphology and the geological conditions in the catchment force a rapid response of the vegetation cover to precipitation decrease and are responsible for relatively low soil stability. Primary productivity in Lake Ohrid is low due to the low nutrient levels (e.g., total phosphorous: 0.15±0.026 mmol m^{-3}, Matzinger et al., 2007). Short distances, rapid response and little dilution through aquatic productivity are excellent preconditions for the reconstructions of biome dynamics using sedimentary OM composition.

While the use of biological markers as proxies for environmental change is well established, we present the first data set of this kind for the Ohrid Basin to improve the interpretation of sedimentary OM compositional changes. We incorporate observations made during the study of sediments from pilot cores taken prior to the 2013 ICDP drilling. Our catchment data then allows us to identify the main OM sources to the Lake Ohrid sediments.

2 Sampling, materials and methods

2.1 Sample collection

Sampling was carried out along the southern and southeastern shores of Lake Ohrid (Fig. 1) in June 2012 and 2013, respectively. We did not sample each component of the ecosystem, but instead focused on the major OM sources. Leaf litter and underlying topsoils (O2 and A horizons) were collected on the Macedonian side of the lake at three sites: under light forest vegetation dominated by small oaks in the vicinity of the Saint Naum karst springs (SN, Fig. 1), from a similar site about 2 km north of Trpejca (TP) and in a high-altitude beech forest of the Galicica National Park (GN). We also sampled one mineral soil (DG, Fig. 1), a deep red Chromic Luvisol (Terra Rossa) that

BGD
12, 12975–13039, 2015

is frequently exposed in gullies or along road cuttings. The sample was taken about 50 cm below the soil surface and about 30 cm below the A-horizon. In contrast to the topsoils, this sample does not contain any significant amounts of fine root material.

At two littoral sites, near the DG site and ~ 2 km north of Pogradec, we collected samples of reed (*Phragmites* spp.). Submerged macrophytes were collected from a small vessel along two transects from 4–16 m water depth off the town of Pogradec and the village of Tushemisht (Albania; Fig. 1) using a small Van Veen bottom sampler (Hydro-Bios, Kiel, Germany). From shallow to deep water, we collected benthic algae (*Cladophora* spp.), one species of pondweed (*Potamogeton perfoliatus*) and 3 species of charophytes (*Characea tomentosa*, *C. gymnophilia*, *C. contraria*).

Lake water samples were collected from two sites (DEEP and Co1202; Fig. 1) by deployment of Niskin Bottles (20 L). The water samples were filtered immediately after collection in the laboratory of the Hydrobiological Institute in Ohrid using an electrical pump and pre-combusted glass fiber filters with a nominal pore size of 0.7 µm. The filters were stored (−20 °C) until freeze-drying in the laboratory at Cologne University.

11 sediment samples were taken from core Lz1120 situated close to the southeastern shores of Lake Ohrid (Fig. 1). The detailed site description and age model are provided by Wagner et al. (2009). Accordingly, our samples cover the time span from 8.65 to 8.05 ka (8647–8049 ± 130 cal years BP), sampled with a time resolution of 60 years. The sediment core sections were stored cold in the repository of the Institute of Geology and Mineralogy at Cologne University (Germany) prior to sub-sampling. Samples were freeze-dried before shipment and stored (−20 °C) prior to analysis. All terrestrial samples and macrophytes were stored cold in the field (4 °C) and then dried (70 °C, 48 h).

2.2 Elemental analysis

Total carbon (TC) and total nitrogen (TN) contents were measured in duplicate (values were < 10 % of the mean) using a CE Instruments NC 2500 elemental analyzer. Total organic carbon (TOC) was determined after acid vapor (HCl) digestion of the carbonate

BGD
12, 12975–13039, 2015

fraction (Yamamuro and Kayanne, 1995). Carbonate contents (assuming all carbonate was as $CaCO_3$) were then calculated from the difference between TC and TOC measurements using the equation $CaCO_3$ = (weight% TC − weight% TOC) · M_{CaCO_3}/M_C (M = molar/atomic mass; $CaCO_3$ = 100, C = 12). Contents of total organic carbon (TOC) and carbonate ($CaCO_3$) are given as percentages of dry weight. The ratio of total organic carbon to total nitrogen (TOC/TN) is given as the molar ratio.

2.3 Lipid analysis

For extraction of the lipid fraction, between 0.5 g (plant matter) and 2 g (sediments) of homogenized sample material was sonicated (3 × 15 min) in a mixture of dichloromethane (DCM) and methanol (9 : 1, *v* : *v*; 10 mL). The total lipid extract (TLE) was concentrated and any water removed by passing it through a Pasteur pipette column packed with anhydrous sodium sulphate. Free and bound acids were then transmethylated by adding a solution of acetyl chloride in methanol (1 : 30, *v* : *v*; 1 mL; 0 °C) and then warming the samples (45 °C, 12 h). The methylated TLEs were dried under nitrogen and re-dissolved in DCM and passed through a column loaded with potassium carbonate to remove excess acetic acid. Finally, N,O-bis-(trimethylsilyl)-trifluoroacetamide with 1 % trimethylchlorosilane was added and the TLE and warmed (65 °C, 30 min) to derivatise compounds with hydroxy groups (e.g., *n*-alcohols, sterols).

Water filtrates were extracted using a Dionex Accelerated Solvent Extraction system (ASE), with DCM and methanol (9 : 1, *v* : *v*) as solvent. Aliquots of the resulting total lipid extracts were separated into aliphatic, aromatic and hetero-compound fractions by column chromatography using deactivated silica (mesh size 60) and elution with hexane, DCM : hexane (2 : 1, *v* : *v*) and methanol, respectively. The polar fractions of the water filtrates were transmethylated and derivatised following the same protocol described above.

Aliquots of the transmethylated and derivatised extracts were injected onto a Trace 2000 Series gas chromatograph fitted with an on-column injector and a fused high-temperature silica column (60 m × 0.25 mm i.d.; 5 %; DB5-HT equivalent; J&W) with

BGD
12, 12975–13039, 2015

helium as the carrier gas (ca. 1.2 mL min^{-1}). A retention gap of deactivated fused silica (1 m × 0.32 mm i.d.) was used at the front of the column. The oven was programmed from 60 to 170 °C at 6 °C min^{-1} after 1 min, then to 315 °C at 2.5 °C min^{-1} and held for 10 min. The GC column was fed directly into the EI source of a Thermoquest Finnigan TSQ7000 mass spectrometer (ionisation potential 70 eV; source temperature 215 °C; trap current 300 µA), operated in Full Data Acquisition mode, (50–600 Thompsons cycled every s) and data was processed using Xcalibur software. Compounds were identified either by comparison of their mass spectra and relative retention indices with those available in the literature and/or by comparison with authentic standards. Quantitative data were calculated by comparison of peak area of the internal standard, 5α(H)-cholestane (spiked onto the samples before extraction), with those of the compounds of interest, using the total ion current chromatogram. The relative response factors of the analytes were determined individually for 36 representative compounds using authentic standards. For analytes for which authentic standards were not available, the response factors for similar compounds of the same class and/or similar structure were used. Reproducibility of similar lipid analyses was determined to be $< \pm 15$ % by (Kiriakoulakis et al., 2000). Data quality was checked regularly with procedural blanks for each extracted sample batch and organic contamination was subtracted from the sample values, although it typically was insignificant ($\ll 1$ % of the sample values). Total lipids were calculated as the sum of all identified compounds from the total ion chromatograms (TIC).

2.4 Statistical methods

Statistical analyses (Multi-dimensional scaling, MDS; Analysis of Similarity, ANOSIM; Similarity Percentages, SIMPER) were conducted on lipid biomarkers, their concentrations being normalised to percentage of total identified lipids ($\%_{lipid}$). The analyses were carried out separately for soils, leaf litters, macrophytes, lake particulate organic matter (POM) and sediment samples from core Lz1120. 78 variables were chosen;

BGD
12, 12975–13039, 2015

these were saturated and branched fatty acids, hydroxy acids, alcohols, *n*-alkanes and amyrins. Where there were zero values, a minimum detection limit was chosen of one half of the lowest recorded concentration, namely 0.001 $\%_{lipid}$ (Yunker et al., 2005). Data were fourth root transformed and screened to confirm a normal distribution using a Draftsman's plot for all variables prior to analyses, which were carried out using PRIMER software (Primer-E Ltd., UK). All quantitative data can be found in the Supplement.

2.5 Compound specific isotope analysis (CSIA)

For compound-specific carbon and hydrogen isotopes analyses, *n*-alkanoic acids (FAs) were isolated from the TLEs. TLEs were first taken up on a small amount of alumina, which was dried and transferred onto a silica column (2.5 g of silica in 25 cm Pasteur pipettes). Fractions were successively eluted using solvent mixtures of increasing polarity (3.5 mL each of *n*-hexane (fraction 1), *n*-hexane/toluene 3 : 1 (fraction 2), *n*-hexane/toluene 1 : 1 (fraction 3), *n*-hexane/ethyl acetate 9.5 : 0.5 (fraction 4), 9 : 1 (fraction 5), 8.5 : 1.5 (fraction 6) and 8 : 2 (fraction 7)). Long-chain FAs ($> C_{20}$) elute in fraction 3 while short-chain FAs ($< C_{20}$) elute in fraction 4. As C_{16} was the dominant FA in many samples, this chain-length separation was useful as comparable concentrations for isotope analyses were achieved for short and long-chain compounds, thus, avoiding bias related to significant differences in signal/peak size.

Stable carbon isotopic compositions of individual lipids were determined using a Thermo Trace Ultra GC linked to a Delta V Advantage isotope ratio monitoring MS (irmMS) by a ConFlo IV interface (Thermo Fisher, Bremen, Germany). Samples dissolved in hexane were injected in splitless mode onto a DB-5 fused silica capillary column (30 m, 0.25 mm ID, 0.25 µm film thickness, J&W Scientific). The injector temperature was 280 °C. The GC temperature was held at 45 °C (1 min), then programmed to 295 °C at 6 °C min^{-1} and held for 15 min. The carrier gas was ultra-high purity grade helium at a constant flow rate of 1.4 mL min^{-1}. The GC column fed directly into a combustion reactor (1000 °C). The combusted compounds then passed through a water separa-

BGD
12, 12975–13039, 2015

tor consisting of a Nafion tube, prior to entering the isotope ratio mass spectrometer. CO_2 reference gas (externally calibrated relative to Vienna Pee Dee Belemnite (VPDB) on a dual inlet mass spectrometer) was automatically introduced into the irmMS in a series of pulses and its $^{13}C/^{12}C$ ratio measured. The accelerating voltage was 3 KV and the trap current and box voltage were set at 0.84 mA and 0.66 V respectively; the electron energy was 124 eV. The irmMS automatically measured the ion intensities of m/z = 44, 45, 46 corresponding to $^{12}C^{16}O_2$, $^{13}C^{16}O_2$, and $^{12}C^{16}O^{18}O$, respectively. Thermo Isodat 3 software automatically computed the $^{13}C/^{12}C$ and $^{18}O/^{16}O$ ratios of each sample peak, referenced to the standard CO_2 gas and its known $^{13}C/^{12}C$ and $^{18}O/^{16}O$ content. Carbon isotopic compositions represent averaged values of duplicate or triplicate analyses. The results are reported in per mil (‰) relative to VPDB international standard. Standards containing FA methyl esters (FAMEs; Schimmelmann, Indiana University, Bloomington, IN, USA) were used to determine instrument precision (< 0.3 ‰) and accuracy (< 0.5 ‰).

Stable hydrogen isotopes of individual fatty acid methyl esters (FAMEs) were measured in duplicate or triplicate using a Thermo Trace Ultra GC linked to a Thermo Delta V+ irmMS (HT voltage 3–5 kV, Trap current 0.75 mA, Box current 0.7 mA) via a Combustion III Interface (Thermo Fisher, Bremen, Germany). Samples dissolved in hexane were injected in splitless mode by a CTC auto sampler onto a DB-5MS UI fused silica capillary column (30 m, 0.25 mm ID, 0.25 µm film thickness, J&W Scientific). The injector temperature was 280 °C. The GC temperature was programmed from 50 to 180 °C at 10 °C min^{-1} and to 300 °C at 3 °C min^{-1} and held for 3 min. Helium flow was 1 mL min^{-1}. The solvent peak was diverted to the FID and H_2 reference gas was initially pulsed into the mass spectrometer. After 7 min the back flush valve directed the split sample via the combustion furnace (1400 °C) into the mass spectrometer and the isotope ratio was measured. Data acquisition was controlled by Thermo Isodat software and raw data was processed using the Isodat dynamic background integration Workspace software. Isotope ratios are given as δ^2H values relative to the reference gas (H_2) calibrated from a reference alkane A4 or FAME F8 mixture with known isotopic

BGD
12, 12975–13039, 2015

values for hydrogen (Schimmelmann, Indiana University, USA). The average standard deviation for duplicate and triplicate analyses of all samples was ±4 ‰.

3 Results and discussion

3.1 Elemental analysis

3.1.1 Leaf litter and soils

Leaf litter samples from the near-shore low-altitude forests (sites SN and TP) have high TOC contents of 43 ± 2 % and TOC/TN ratios of ~ 27 ± 2 (Table 1). TOC contents of the Leptosol O- and A-horizons at SN and TP range from 7.5 to 11 %, while their TOC/TN ratios vary little around 17 (Table 1). The TOC/TN ratio of the high-altitude Leptosol (GN) is slightly lower, with a value of 15.3 ± 0.8. For all Leptosols, carbonate contents are low and vary between 5 and 8 %. The B-horizon of the Chromic Luvisol (Terra Rossa; DG) has low TOC and carbonate contents of 0.9 and < 0.5 %, respectively, within reported ranges for this soil type in the Mediterranean (e.g., Costantini et al., 2013: TOC 0.5 %, $CaCO_3$: 0.5 %, n = 48). The TOC/TN ratio of the Terra Rossa soil is 11.4 ± 0.8, which is also significantly lower than the Leptosols (Table 1).

3.1.2 Macrophytes

The macrophyte samples can be separated into two types of plant that (a) do precipitate carbonate, i.e., *Characeae* spp., and (b) do not, i.e., *Cladophora* spp., *Potamogeton* spp., *Cladophora* spp., *Potamogeton* spp. and the leaves of *Phragmites* spp. Plants from group (b) have similar TOC contents (42 ± 2 %); TOC/TN ratios are also similar (13.5 ± 0.3 ; Table 2). The two specimens of *Characeae* (*Chara tomentosa*, *Chara gymnophyla*) have high amounts of carbonate (66 ± 7 %), diluting the TOC contents to 10 ± 0.3 %. The TOC/TN ratios are higher than those of the other macrophytes: 17.8 ± 1.2. High carbonate contents of > 70 % are common for charophytes in freshwa-

BGD
12, 12975–13039, 2015

ter systems (see Apolinarska et al., 2011 and references therein). Królikowska (1997) reports calcium contents of 234 and 246 mg g^{-1} dry weight for *Chara tomentosa* and *Chara contraria* from a shallow Polish lake, or carbonate contents of 59 ± 4 % and 61 ± 2 %, respectively, assuming that all calcium is present as carbonate, close to our value for *Chara tomentosa* (61.5 %).

3.1.3 Sediments

Carbonate contents of the Lz1120 sediments range from 20 to 56 % and TOC from 1.5 to 2.3 % (Fig. 2). The carbonate record of Lake Ohrid appears to be controlled by temperature and terrestrial run-off, with precipitation and production of largely endogenic carbonate occurring mostly during the summer (Wagner et al., 2008; Vogel et al., 2010) and relying on the supply of calcium ions and nutrients from the catchment. Accordingly, minima in sedimentary carbonate represent periods of drier and cooler climate. Between 8.8 and 7.9 ka the Lz1120 carbonate record features two pronounced minima at around 8.3 and 8.15 ka that appear to correspond to phases of the 8.2 ka event (Fig. 2) as documented in sediment records from the North Atlantic (MD99-2251) and Greenland ice cores (GISP 2; Ellison et al., 2006). TOC decreases from 2.3 to a minimum of 1.5 % at ca. 8.3 ka and remains below 2 % thereafter. Carbonate and organic carbon contents appear to co-vary apart from in the three youngest samples between 8.05 and 7.9 ka and the sample separating the two carbonate minima at 8.23 ka. In the remaining samples, TOC and carbonate correlate closely (R^2 = 0.86). TOC/TN ratios range from 7 to 10.7, with values > 10 between 8.9 and 8.3 ka (average: 10.5 ± 0.2) and < 10 thereafter (average: 8.1 ± 0.7). Higher TOC/TN values generally coincide with higher organic carbon contents (R^2 = 0.91). When TOC is plotted against TN, however, the samples are clearly separated into two groups (Fig. 2, insert): samples from before and after 8.3 ka show similar concentrations of TN but significantly different concentrations of TOC, with lower TOC relative to TN after 8.3 ka. Before 8.3 ka, there is a strong linear relationship between TOC and TN (R^2 = 0.94), with a *y* axis intercept of 0.057 % TN for 0 % TOC, suggesting that around a quarter of the nitrogen is inorganic. The

BGD
12, 12975–13039, 2015

amount of organic nitrogen (N_{org}) that results from this assumption leads to an average TOC/N_{org} ratio of 13.6 for the samples before 8.3 ka. After 8.3 ka, the correlation between TOC and TN disappears, implying that higher nitrogen concentrations do not generally result from the supply of nitrogen-rich OM, but from variable amounts of inorganic nitrogen (N_{in}) such as ammonium (NH_4^+). The implications for the interpretation of the TOC/TN record of Lz1120 are discussed below (Sect. 4.1 Assessing aquatic and terrestrial OM supply).

3.2 Lipid biomarkers

3.2.1 Leaf litter and topsoils

Biomarker concentrations

Leaf litter under both types of vegetation, low-altitude oak-dominated forest (sites SN, TP) and high-altitude beech forest (GN) contain very similar total amounts of lipids: ca. $458 \pm 63\,\mu g\,g^{-1}$ dry weight ($n = 4$). Lipid contents of the topsoils are approximately 7× lower, with an average of $55 \pm 21\,\mu g\,g^{-1}$ dry weight ($n = 6$) for the Leptosols.

There are compositional differences in the major lipid compound classes, between leaf litter and corresponding topsoils and between high-altitude and low-altitude sites (see Fig. 3 and Table 2). Lipids of the near-shore oak-dominated leaf litter (sites SN, TP) are dominated by saturated FAs that account for $35 \pm 1.4\,\%_{lipids}$, while the other major compound classes, i.e. mono- and poly-unsaturated fatty acids (MUFAs, PUFAs) and sterols, vary between 8 and $20\,\%_{lipids}$. PUFAs and MUFAs are present in similar proportions, 10.5 ± 1.1 and $8.6 \pm 2.4\,\%_{lipids}$, respectively. In high-altitude beech-dominated litter (GN), FAs make up only $24\,\%_{lipids}$ and the proportions of MUFAs and PUFAs are considerably higher, 22 and $18\,\%_{lipids,}$ respectively. Sterols make up $23.6\,\%_{lipids,}$ with β-sitosterol ($17\,\%_{lipids}$) and β-sitostenone ($5\,\%_{lipids}$) together accounting for 96 % of the total sterols. β-Sitosterol is also the dominant sterol in low-lying oak-dominated litter (SN, TP; $10.7 \pm 0.4\,\%_{lipids}$). In SN leaf litter, the pentacyclic triter-

BGD
12, 12975–13039, 2015

penoid, taraxasterol is also abundant (11.7 ± 1.1 $\%_{lipids}$, on average). This compound occurs in exceptionally high amounts in *Lapsana communis* or nipplewort (Fontanel et al., 1998), which is an element of the "Riverine Forest" vegetation in the area of the St. Naum springs (Matevski et al., 2011). Other members of the Asteraceae family such as *Jurinea taygetea* that are present in Macedonia (Ministry of Environment and Physical Planning, 2003) have also been reported to have a high abundance of taraxasterol (Mikolajczak and Smith, 1967; Muley et al., 2009). The absence of taraxasterol in the topsoil samples underlying the leaf litter at sites SN and TP suggests that it is quickly degraded. Taraxasterol was absent in the litter and soil samples at GN.

The proportions of the major compound classes observed in leaf litter are different to the underlying topsoils. While the relative amounts of FAs remain similar (24–29 $\%_{lipids}$), the MUFAs increase in relative abundance from leaf litter to soil from ca. 9 to 21 $\%_{lipids}$ at TP and SN and from 22 to 26 $\%_{lipids}$ at GN with *n*-$C_{18:1}$ (*cis*-9) being the dominant MUFA. Small amounts of *n*-$C_{20:1}$ (*cis*-9) MUFA might derive from collembolans (springtails), small detritivorous and microbivorous hexapods feeding on nematodes as well as fungi in leaf litter (Ruess et al., 2005). PUFAs, on the other hand, decrease from leaf litter to soil in relative abundance at all sites, most notably at GN, to between 4 and 6 $\%_{lipids}$. The dominant PUFA in all leaf litter samples is $C_{18:2}$. Leaf litter at sites TP and GN contained $C_{18:2}$ only, albeit in higher amounts than at site SN with 11 $\%_{lipids}$ (TP) and 18 $\%_{lipids}$ (GN) vs. 8 $\%_{lipids}$ (SN). $C_{18:3}$ occurs only at site SN where it accounts for 2 $\%_{lipids}$. For $C_{18:2}$, this pattern is also preserved in the corresponding soils. The proportion of PUFA is also higher in the soil sample affected by white rot (TP-F), which is the only soil sample where we detected a small amount of $C_{18:3}$ and, notably eicosapentaenoic acid (EPA; $C_{20:5}$). The latter probably has a fungal source as some soil fungi such as *Mortierella alpina* or plant pathogens such as *Pythioum ultimum* are known to biosynthesize EPA (Shimizu et al., 1988; Ghandi and Weete, 1991).

The higher amounts of *n*-$C_{18:1}$ (*cis*-9) MUFA in the soils (58 % of all unsaturated FAs at TP and SN, up to 71 % at GN) are likely to derive from root suberin in addition to

BGD
12, 12975–13039, 2015

cutin. Besides *n*-C_{16} FA and *n*-C_{18} FA, the *n*-$C_{18:1}$ MUFA is one of the main monomers synthesized de novo to form both cutin and suberin (Mertz and Brutnell, 2014).

The relative amount of steroids also decreases from leaf litter to soil. At GN, their relative abundance halves compared to the leaf litter (24 to 12 $\%_{lipids}$). At TP and SN the decrease is less pronounced, from 15 to 13 $\%_{lipids}$. The main sterol in both leaf litter and topsoils is β-sitosterol accounting for 60 to 80 % of the total sterols. Other steroids include stigmastanol, cholesterol, stigmasterol, campesterol, brassicasterol, ergosterol and β-sitostenone (see Table A1 for IUPAC names), all of which are proportionally more abundant relative to β-sitosterol in the topsoils than in the leaf litter samples. The exception is β-sitostenone, which accounts for 12 to 21 % of the total steroids in the leaf litter samples and most likely arises from early plant litter breakdown and has been reported, e.g., in the common wood-decaying fungus, *Xylaria* spp. (Wang et al., 2014). Finally, the leaf litter TLEs from all sites contain ca. 3 $\%_{lipids}$ α-tocopherol, which functions as an antioxidant in plants (e.g., Chevolleau et al., 1993) and has also been identified in fungi (e.g., Reis et al., 2011). In the topsoils, the amount of α-tocopherol drops to ca. 0.4 $\%_{lipids}$.

A notable difference in the total lipid composition between leaf litter and underlying soils is the significantly higher proportion of *n*-alcohols in the latter. *n*-Alcohols account for 3.5 ± 0.5 $\%_{lipids}$ in leaf litter at SN and TP and 6.6 $\%_{lipids}$ at GN. However, their proportions in the soils are 4 and 2.5-times higher, respectively.

Minor compound classes present in leaf litter and soils include hydroxy acids, *n*-alkanes and branched FA. Hydroxy acids (OH-FA) are more abundant at SN (4.0 ± 1.0 $\%_{lipids}$) than TP (1.2 $\%_{lipids}$) and GN (0.9 $\%_{lipids}$). In leaf litter at SN, relative concentrations of α-hydroxy acids (α-OH-FA) are ca. 10× higher than ω-hydroxy acids (ω-OH-FA absent in TP sample), while leaf litter at GN is dominated by ω-OH-FA. However, soils from all sites show similar relative amounts of ω- and α-OH-FAs (5–6 $\%_{lipids}$). The substantial increase in the amounts of ω-OH-FAs from litter to soil by an order of magnitude and the chain-length range from C_{16} to C_{26} (site GN: C_{16}–C_{28}) suggest their source is suberin, a protective biopolymer mainly found in the periderm

BGD
12, 12975–13039, 2015

of plant root and stem tissues, but also in bundle sheaths of grasses (Pollard et al., 2008; Molina et al., 2006). *n*-Alkanes account for 5–6 $\%_{lipids}$ in the leaf litter samples, but only 3 $\%_{lipids}$ in the soil samples at all three sites. The proportions of branched FAs increase by an order of magnitude from 0.2 to 2.7 $\%_{lipids}$ and 0.1 to 1.5 $\%_{lipids}$ at SN and GN, respectively; they are absent at TP. There is a difference in the composition of branched FAs between litter and topsoil samples. While the litter samples mainly contain *iso*- and *anteiso*-branched C_{15} FA as well as *iso*-C_{16} FA, the topsoil samples additionally contain *iso*- and *anteiso*-C_{17} FA as well as 10-methyl hexadecanoic acid. Finally, α,ω-dicarboxylic acids (α,ω-DiFAs) occur almost exclusively in the soil samples, the exception being one leaf litter sample from site SN where α,ω-DiFAs were detected in small amounts (0.3 $\%_{lipids}$). In all other leaf litter samples, α,ω-DiFAs were not detectable. By contrast, α,ω-DiFAs accounted for 1 $\%_{lipids}$ (SN) and 0.7 $\%_{lipids}$ (TP) in the low-altitude soils and for 0.4 $\%_{lipids}$ in the high-altitude sample (GN). As for the ω-OH-FAs, their occurrence with a chain length range of C_{16}–C_{26} strongly suggest that the main source of the α,ω-DiFAs is suberin.

Carbon number distributions of *n*-alkyl compounds

Chain length distributions of *n*-alkyl compounds (saturated *n*-FA, *n*-alcohols, α- and ω-OH-FA and *n*-alkanes) show subtle differences between high-altitude beech-dominated (GN) and near-shore low-lying oak-dominated leaf litters (TP, SN), and between litter and underlying soils, which could nevertheless be useful in tracing provenance of OM in the lake sediments. The main *n*-alkanoic acid in both leaf litter and topsoils is C_{16} FA. At TP and SN, the leaf-litters have a trimodal chain-length distribution, with long-chain and mid-chain length C_{30} FA and C_{22} FA, respectively, being the other modes (Fig. 3). This trimodal distribution is more pronounced at GN, with C_{22} FA being the mid-chain mode, while the C_{28} FA is the long-chain mode. The proportion of mid-chain compounds, in particular, the amounts of C_{22}- and C_{24}-FA increase significantly in the low-altitude topsoils (TP, SN), relative to the overlying leaf litters (Figs. 3 and 4). Accordingly, the average chain-length (ACL; Eq. 1) between C_{22} and C_{26}-FA shifts from 24.2 to 23.6

BGD
12, 12975–13039, 2015

between litter and topsoil.

$$\mathrm{ACL} = (22 \cdot C_{22} + 24 \cdot C_{24} + 26 \cdot C_{26})/(C_{22} + C_{24} + C_{26}). \quad (1)$$

The *n*-alcohols show pronounced bimodal distributions of mid- and long-chain compounds. In GN leaf litter C_{20} and C_{28} *n*-alcohols (OH) dominate, while at TP and SN C_{24} OH and C_{30} OH are mid and long-chain modes, respectively. The bimodal character results from the *n*-alcohols deriving from two major sources: (a) cuticular wax esters, with chain lengths of C_{26} and C_{28} or, in some cases, C_{30} and C_{32} (e.g., Samuels et al., 2008 and references therein) and (b) suberin, with C_{22} and C_{24} OHs being the main monomers (Molina et al., 2006).

Comparison of the relative abundances of individual FAs and OHs in the two samples from site TP reveals the effect of white rot on chain-length distribution (Fig. 4b and c). Fungal biomass contribution and breakdown of plant material appears to increase the proportion of short-chain C_{16} and C_{18} FA and of C_{30} FA (Fig. 4b) as well as the proportions of C_{30} and C_{32} OH, relative to mid- and short-chain OHs (Fig. 4c).

Chain lengths of ω-hydroxy acids in all leaf litter samples range from 16 to 22 but are dominated by short-chain C_{16} ω-OH-FA (Fig. 3). This distribution is typical for cutin monomers (Matzke and Riederer, 1991), the lipid polymer being part of the protective hydrophobic layer of plant cell walls (Pollard et al., 2008). In the soil samples, ω-OH-FAs range from C_{16} to C_{26}, the dominant compounds being C_{22} ω-OH-FA and C_{24} ω-OH-FA, which together account for $\sim 50\,\%$ of the total ω-OH-FA in the TP and SN soils and 65 % of the total ω-OH-FA in the GN topsoil, where the proportion of C_{24} ω-OH-FA is higher. C_{22} ω-OH-FA and C_{24} ω-OH-FA typically are the main ω-OH-FAs in suberin from *Quercus robur* L. and *Fagus sylvatica* L. (Matzke and Riederer, 1991) or *Quercus suber* (Graça and Santos, 2007) and a similar ω-OH-FA distribution has been reported for an oak forest soil by Nierop et al. (2005). α-Hydroxy acids range from C_{22} to C_{24} in GN litter and C_{15} to C_{26} in TP and SN litters, with C_{24} α-OH-FA being dominant, followed by C_{22} α-OH-FA; there are also high abundances of odd-numbered

BGD
12, 12975–13039, 2015

α-OH-FAs, C_{23} and C_{25} in particular. The distribution of α-OH-FAs is similar in the underlying soils.

n-Alkanes in the leaf litter samples (sites TP, SN, GN) range from *n*-C_{23} to *n*-C_{31} and reveal a clear compositional difference between high-altitude beech-dominated and low-lying oak-dominated leaf litters (Fig. 3): the main *n*-alkane at GN is *n*-C_{29} while litter at SN and TP almost exclusively contains *n*-C_{27}, accounting for 90 % of the total *n*-alkanes. Thus, the average chain length (*n*-C_{27} to *n*-C_{31}; $ACL_{27–31}$) is 28.9 for the GN site and 27.1 at TP and SN. In the soils, *n*-alkane chain lengths range from C_{23} to C_{33}. The dominant *n*-alkane in all low-altitude topsoil samples is *n*-C_{29}. Compared to the leaf litter samples the ratio of *n*-C_{29} relative to *n*-C_{31} (C_{29}/C_{31} = *n*-C_{29}/(*n*-C_{29} + *n*-C_{31})), decreases from 0.78 in leaf litter to 0.63 in the corresponding topsoils at SN, TP. In the sample affected by white rot (TP-F) this ratio is even lower (0.56). In GN leaf litter *n*-C_{31} was absent. Notably, *n*-alkanes in the soil at site GN show a bimodal distribution, with *n*-C_{31} and *n*-C_{27} being the main *n*-alkanes and the C_{29}/C_{31} ratio is 0.36.

The α,ω-dicarboxylic acids (α,ω-DiFAs) in the topsoils reveal chain-length distributions that are similar to those of the ω-hydroxy acids, i.e. bimodal, with peaks at C_{16} and C_{22}. Notably, the increased proportions of C_{24} relative to C_{22} ω-OH-FA that is observed in the high-altitude soil when compared to the low-lying soils is reflected in the DiFA chain-length distribution confirming that both ω-OH-FAs and α,ω-DiFAs most likely derive from suberin. The presence of α,ω-DiFAs in roots but not in leaves and stems of land plants, led Mendez-Millan et al. (2011) to conclude that α,ω-DiFAs represent subterranean biomass.

3.2.2 Mineral soil (Terra Rossa)

As for TOC, the mineral soil (DG) contains the lowest amount of lipids (1.3 $\mu g\,g^{-1}$ dry weight), an order of magnitude lower than the lipid content of the topsoils. Almost half (48 $\%_{lipids}$) are *n*-alcohols, followed by unsaturated FAs (20 $\%_{lipids}$), saturated FAs (15 $\%_{lipids}$) and steroids (11 %), with β-sitosterol being the dominant sterol (9 $\%_{lipids}$). Minor components include *n*-alkanes (3.5 $\%_{lipids}$), OH-FAs (1.4 $\%_{lipids}$) and branched

BGD
12, 12975–13039, 2015

FAs (0.6 $\%_{lipids}$), with the relative amounts of the *n*-alkanes being slightly higher, and of branched FA and OH-FA lower than in the topsoils. α,ω-DiFAs were absent in the mineral soil and the only "other" compound is β-amyrin (1.2 $\%_{lipids}$).

The fundamental difference in bulk lipid composition between the mineral soil and the topsoils is the significantly higher proportions of *n*-alcohols and the very low amounts of saturated FAs which are even lower than those of the unsaturated FAs. The latter suggests that a large proportion of the unsaturated FA in the mineral soil is produced in situ, with the dominant *n*-$C_{18:1}$ (*cis*-9) MUFA (45 % of unsaturated FA) most likely to derive from suberin.

The *n*-alcohols have a bimodal chain-length distribution peaking at 28 and 24, with *n*-C_{28} OH accounting for 45 % and *n*-C_{24} OH for 19 % of all *n*-alcohols. The saturated *n*-alkanoic acids are dominated by short- and mid-chain FA, with *n*-C_{16} FA and *n*-C_{22} FA being the most abundant compounds (36 and 17 % of all saturated *n*-FA, respectively). As in the topsoils, the dominant ω-OH-FA is the C_{22} compound, the only α-OH-FA is the C_{24} homologue. Chain lengths of the *n*-alkanes range from 23 to 33, with *n*-C_{31} and *n*-C_{29} being dominant compounds and being present in almost equal amounts (C_{29}/C_{31} = 0.49) accounting for 68 % of the total *n*-alkanes.

3.2.3 Macrophytes

Submerged macrophytes contain between 0.2 and 1.1 mg g^{-1} dry wt. of lipids, which is in the same range as the leaf litter. Highest concentrations are found in *Cladophora* spp. (1.07 ± 0.33 mg g^{-1}). *Potamogeton* spp. and *Characeae* spp. contain lower amounts (0.22 ± 0.13 mg g^{-1} and 0.53 ± 0.34 mg g^{-1}, respectively), which is likely due to a higher proportion of supportive tissue in the latter and, in case of *Characeae* spp., carbonate incrustations. Sub-aquatic and sub-aerial parts of *Phragmites* spp. were analysed separately; lipid concentrations in the root and stem (sub-aquatic) are in a similar range to the submerged macrophytes (0.44 and 0.34 mg g^{-1}, respectively). The highest lipid concentrations were in the (sub-aerial) *Phragmites* spp. leaves (1.7 ± 0.3 mg g^{-1}).

BGD
12, 12975–13039, 2015

The macrophyte lipids are dominated by unsaturated and saturated fatty acids that, together, account from 64 $\%_{lipids}$ (*Potamogeton*) to 95 $\%_{lipids}$ (*Cladophora*). Unsaturated FAs dominate, with slightly higher proportions in *Phragmites* sp. leaves (59 $\%_{lipids}$) and *Characeae* spp. (57 $\%_{lipids}$) and lower proportions in *Potamogeton* spp. (41 $\%_{lipids}$) and the *Phragmites* sp. roots (48 $\%_{lipids}$). The $C_{18:2}$ PUFA is the dominant unsaturated FA in the *Phragmites* sp. stem (21 $\%_{lipids}$) and roots (27 $\%_{lipids}$), while in the leaves it is the $C_{18:3}$ PUFA (48 $\%_{lipids}$). The latter also dominates in *Potamogeton* sp. (23 $\%_{lipids}$). $C_{16:1}$ (*cis*-9) MUFA is most abundant in *Cladophora* sp. (29 $\%_{lipids}$), which also contains the highest amounts of $C_{18:1}$ (*cis*-9) MUFA (8 $\%_{lipids}$). $C_{16:1}$ (*cis*-9) MUFA was also present in traces in *Phragmites* stems (13 $\%_{lipids}$) but absent in roots and leaves.

Saturated *n*-alkanoic acids have highest relative abundance in *Cladophora* spp. (45 $\%_{lipids}$) and lowest concentrations in *Phragmites* sp. leaves (15 $\%_{lipids}$). They are dominated by C_{16} FA, which accounts for about three quarters of all saturated FA, with lower values only in the *Phragmites* stem and root (67 and 55 % of saturated FA, respectively), where there are slightly elevated amounts of C_{20} FA and C_{24} FA. The remaining compounds are mainly sterols, accounting for 3.6–12 % of the total lipids and with highest amounts in *Potamogeton* spp. (33 $\%_{lipids}$) and elevated proportions in the *Phragmites* sp. root and stem (12 and 11 $\%_{lipids}$, respectively). The main sterol present in all samples is β-sitosterol followed by stigmasterol (absent in *Cladophora* sp.). Small amounts of cholesterol (0.1–2.3 $\%_{lipids}$) were detected in all samples except for the *Phragmites* sp. stem.

n-Alcohol concentrations are generally very low (< 1.5 $\%_{lipids}$), with the exception of the *Phragmites* leaves where long-chain C_{28} OH and C_{30} OH account for 19 % of the total lipids and likely to derive from cuticular waxes (Samuels et al., 2008). In most samples, hydroxy acids are either absent (*Characeae* spp.) or detected in small amounts of less than 0.4 $\%_{lipids}$ (*Cladophora* spp., *Potamogeton* spp., *Phragmites* spp. leaves). Higher amounts were detected in the *Phragmites* stem and root: 1.4 and 3.5 $\%_{lipids}$, respectively. Thus, *Phragmites* spp. roots, in particular, are a potential macrophytic source for sedimentary α- and ω-OH-FA. As in leaf litter, the amount of α-OH-FA is

BGD
12, 12975–13039, 2015

higher than the amount of ω-OH-FA in all samples where OH-FAs are present. The α-OH-FA chain-length distribution is bimodal in all *Phragmites* spp. tissues, with α-C_{24} OH-FA dominant followed by the α-C_{20} OH-FA. In *Potamogeton* spp. and *Cladophora* spp. α-C_{24} OH-FA dominates, followed by α-C_{22} OH-FA, and only *Potamogeton* spp. contained a small amount of α-C_{16} OH-FA. The main ω-OH-FA is the ω-C_{24} OH-FA compound, which is present in *Potamogeton* spp. (traces) and the *Phragmites* spp. stem and root samples (0.2 and 0.9 $\%_{lipids}$, respectively). The latter also contain ω-C_{22} OH-FA, ω-C_{26} OH-FA and ω-C_{20} OH-FA. Although ω-C_{16} OH-FA was not detected, this distribution suggests that the ω-OH-FA in *Phragmites* spp. also derive from suberin, which is a known biopolymer in *Phragmites australis* (Soukup et al., 2007).

n-Alkanes were either absent (*Characeae*, *Phragmites* root and stem) or found in very low concentrations, e.g., 0.25 $\%_{lipids}$ in *Phragmites* sp. leaves (dominated by *n*-C_{29}, $ACL_{23–31}$ = 28.3) and 1 $\%_{lipids}$ in *Potamogeton* spp. (dominated by *n*-C_{25}, $ACL_{23–31}$ = 25.6). The differences in chain-length distributions between *Potamogeton* spp. and the leaves of *Phragmites* sp. are consistent with observations made by Ficken et al. (2000) on the *n*-alkane composition of macrophytes from lakes on Mt. Kenya. There, *n*-alkanes produced by submerged macrophytes were dominated by mid-chain compounds (C_{23}, C_{25}), whereas *n*-alkanes produced by emergent macrohpytes were dominated by long-chain compounds (> C_{29}) as in land plants. Ficken et al. (2000) suggested a proxy (Eq. 2) to determine varying contributions from submerged and emergent macrophytes defined as:

$$P_{aq} = (n\text{–}C_{23} + n\text{–}C_{25})/(n\text{–}C_{23} + n\text{–}C_{25} + n\text{–}C_{29} + n\text{–}C_{31}), \quad (2)$$

with values between 0.1 and 0.4 suggested to correspond to emergent macrophytes and values between 0.4 and 1 to submerged macrophytes. Accordingly, the P_{aq} value of 0.78 for *Potamogeton perfoliatus* in Lake Ohrid matches the values reported by Ficken et al. (2000) for *Potamogeton thumbergii* (0.73 and 0.92) while the value for *Phragmites* leaves (0.24) does fall in the suggested range for emergent macrophytes.

BGD
12, 12975–13039, 2015

Other macrophyte lipids include α-tocopherol and β-sitostenone. In the *Phragmites* sp. samples, the concentration of α-tocopherol is high in the leaves (13 µg g^{-1}, 0.75 %$_{lipids}$) and lower in the stem and roots (0.4 µg g^{-1}, 0.1 %$_{lipids}$). By contrast, proportions of β-sitosterol and β-sitostenone are higher in stem and root and reflect the requirement of different cell membrane properties and, perhaps, a demand of moderately antibacterial compounds (Nair et al., 2012; Bumrela and Naik, 2011).

3.2.4 Lake water filtrates

The total lipid composition of the water filtrates was not determined, as extracts had previously been separated into non-polar and polar fractions. Here we report the results from analyses of the polar components that include fatty acids, alcohols and steroids. These were dominated by short-chain FAs (C_16 FA and C_{18} FA), accounting for 27 % of polar lipids (%$_{polar\ lipids}$), C_{18} MUFAs (21 %$_{polar\ lipids}$) and some sterols (20 %$_{polar\ lipids}$), mainly cholesterol (8 %$_{polar\ lipids}$), sitosterol (6 %$_{polar\ lipids}$) and stigmastanol (5 %$_{polar\ lipids}$). Minor polar compounds were $C_{18:2}$ PUFA (7 %$_{polar\ lipids}$), *n*-alcohols (4 %$_{polar\ lipids}$), mid- and long-chain *n*-FAs (3 %$_{polar\ lipids}$), branched FAs (2 %$_{polar\ lipids}$) and OH-FAs (1.3 %$_{polar\ lipids}$). The proportion of $C_{18:2}$ PUFA increased with water depth near site Co1202, from 4 to 12 %$_{polar\ lipids}$ suggesting that most recently produced labile OM had sunk to depth at the time of sampling. The methyl ester of the pigment β-apo-4'-carotenoic acid (neurosporaxanthin, 0.8 %$_{polar\ lipids}$) and stigmast-3,5-dien-7-one (0.7 %$_{polar\ lipids}$) were present only in the water filtrates. Long-chain *n*-alkanoic acids and *n*-alcohols were detected in trace amounts, only. Notably, the *n*-alcohol distribution in the water filtrates suggests a bacterial source (Fig. 3b). Yang et al. (2014) observed a very similar *n*-alcohol distribution in *Erythrobacter* sp. isolated from the South China Sea. Albaigés et al. (1984) noted that C_{18} OH and C_{22} OH dominated the free and bound *n*-alcohol fraction in lacustrine sediments from Spain and assigned them to bacterial inputs.

BGD
12, 12975–13039, 2015

3.2.5 Sediments

Total lipid contents of sediments from core Lz1120 range from 7.6 to 79 $\mu g\,g^{-1}$, with an average of 32 $\mu g\,g^{-1}$. With regard to the major lipid compound classes, there are clear compositional differences between the samples with low and high carbonate contents, i.e. between the samples dated to 8.29, 8.17 and 8.11 ka, representing cool, dry episodes associated with the 8.2 ka event, and those from the rest of the investigated time slice. In particular, the proportion of *n*-alkanoic acids is significantly lower in the samples from 8.17 and 8.11 ka compared to the high-carbonate samples (16 vs. 40 $\%_{lipids}$, on average), while the proportions of sterols and *n*-alcohols are higher (24 vs. 15 $\%_{lipids}$ and 37 vs. 21 $\%_{lipids}$, respectively). In the sample from 8.29 ka, both *n*-alkanoic acids (27 $\%_{lipids}$) and *n*-alcohols (18 $\%_{lipids}$) are present in lower amounts but similar proportion relative to each other as in the high-carbonate samples (see "Supplement").

The concentrations of OH-FAs range from 1 to 6.7 $\%_{lipids}$, with averages of 3.3 and 4.6 $\%_{lipids}$ for low- and high-carbonate samples, respectively. These values are similar to those of the topsoil (average: 5.7 $\%_{lipids}$) and leaf litter samples (average: 2.5 $\%_{lipids}$), but significantly higher than in the macrophytes, with the exception of *Phragmites* stems (1.4 $\%_{lipids}$) and roots (3.5 $\%_{lipids}$). As in the soils, but unlike the leaf litters and macrophytes, the majority of the OH-FA in the sediments are ω-OH-FA, except at 8.17 ka where α-OH-FAs dominate (2.1 vs. 1.1 $\%_{lipids}$). Branched FAs account for 0.9 $\%_{lipids}$ on average in the high-carbonate samples. Of the low-carbonate samples, the sample at 8.11 ka shows an exceptionally high value of 2.5 $\%_{lipids}$ while the sample at 8.29 ka contains the lowest amount of branched FAs of all sediment samples (0.2 $\%_{lipids}$). *n*-Alkane concentrations are more than twice as high in the three low-carbonate samples than in the high-carbonate samples (3.3 vs. 1.5 $\%_{lipids}$).

In contrast to macrophytes, leaf litter and soils, the early Holocene sediment samples contain almost no unsaturated fatty acids. The only detectable MUFA is $C_{18:1}$ (*cis*-9) accounting for about 0.1 to 0.5 $\%_{lipids}$, if present. PUFAs are not preserved in the

BGD
12, 12975–13039, 2015

sediments. On the other hand, the C_{21}–C_{33} methyl ketones were identified only in the sediments (0.1 to 1.1 $\%_{lipids}$; with the exception of C_{27} in SN leaf litter).

Other compounds (Table 3) account for 17 % of the total lipids in both high- and low-carbonate samples. These include 17β(H),21β(H)-bishomohopanoic acid (9.3 and 6.1 $\%_{lipids}$ in high- and low-carbonate samples), 1,15-triacontadiol (C_{30} 1,15-diol) and 1,15-dotriacontadiol (C_{32} 1,15-diol) (together 2.8 and 3.4 $\%_{lipids}$), 1,15(ω16)C_{30} keto-ol (1.0 and 1.3 $\%_{lipids}$), tetrahymanol (0.7 and 1.5 $\%_{lipids}$), 17β(H),21β(H)-bishomohopanol (0.6 and 1.6 $\%_{lipids}$), β-amyrin (0.7 and 1.2 $\%_{lipids}$) and small amounts of *iso*- and *anteiso*-branched C_{15} OH (< 0.5 $\%_{lipids}$). α-Tocopherol was also present in the sediments in low amounts of 0.7 and 0.4 $\%_{lipids}$ in both high- and low-carbonate samples. A number of compounds appear in the sediments that are absent in the terrestrial materials and the macrophytes. Apart from the methyl ketones, these include steroids (coprostanol, epicholestanol, epicoprostanol, cholestanol, 24-methyl-5α(H)-cholestan-3β-ol, 24-ethyl-5α(H)-cholest-22(E)-en-3β-ol, dinosterol, dinostanol, lanosterol, *iso*- and *anteiso*-branched C_{15} OH, C_{30} 1,15-diol and C_{32} 1,15-diol, 1,15-(ω16)-C_{30}-keto-ol, tetrahymanol, 17β(H),21β(H)-bis-homohopanol, 17β(H),21β(H)-homohopanoic acid and 17β(H),21β(H)-bis-homohopanoic acid. While most of these compounds are minor components (< 2 $\%_{lipids}$), the long-chain diols, lanosterol and 17β(H),21β(H)-bishomohopanoic acid, on average, account for 3, 4 and 8 $\%_{lipids}$, respectively. The absence of these compounds in the modern terrestrial samples and most of the water filtrates, only the 40 m sample from site Co1202 contains a small amount of lanosterol (0.2 $\%_{lipids}$), suggests they are largely formed or biosynthesized in situ. A bacterial origin in the surface sediment for 17β(H),21β(H)-bis-homohopanoic acid, 17β(H),21β(H)-homohopanoic acid and 17β(H),21β(H)-bis-homohopanol as well as for the branched C_{15} OH seems most likely. Epicholestanol concentrations correlate well with those of 17β(H),21β(H)-bis-homohopanoic acid in the high-carbonate samples (R^2 = 0.89), suggesting that it also originates from a bacterial process for example through reduction of cholesterol (in low-carbonate samples 17β(H),21β(H)-bis-homohopanoic acid appears less well preserved). Although long-chain diols are frequently found in sed-

BGD
12, 12975–13039, 2015

iments, their sources are not fully known. However, they have been found in marine as well as freshwater eustigmatophytes (Volkman et al., 1992, 1999), with the C_{32} 1,15-diol dominating in the marine environment and the C_{30} 1,15-diol dominating in the freshwater environment. We therefore assume that the diols found in Lake Ohrid sediments derive from this microalgal source.

Although not observed in the water filtrates, dinosterol and dinostanol are most likely to derive from organisms living in the water column, in particular dinoflagellates (Robinson et al., 1987). While C_{28} sterols such as 24-methyl-5α(H)-cholestan-3β-ol are often ascribed to diatoms, C_{29} sterols such as 24-ethyl-5α(H)-cholest-22(E)-en-3β-ol are assumed largely to derive from a terrestrial source (Xu et al., 2006), although we did not find the latter in any of our modern samples. Finally, tetrahymanol likely derives from ciliates living at the sediment–water interface. (Schwalb et al., 2013).

The distributions of *n*-alkanoic acids reveal significant differences in chain length between samples with high and low carbonate contents. The input of long-chain *n*-alkanoic acids from terrestrial plant waxes appears strongly reduced relative to short-chain C_{16}-FA and mid-chain C_{22}- and C_{24}-FAs during periods of reduced or diluted carbonate sedimentation. By contrast, the chain-length distribution of *n*-alcohols shows rather subtle differences that, in fact, result from the depletion of long-chain *n*-alcohols in one sample, only (8.29 ka, Fig. 5). *n*-Alkanes show a unimodal distribution peaking at *n*-C_{29} and do not show a significant difference between high- and low-carbonate samples. *n*-C_{31} is slightly more abundant relative to *n*-C_{29}. The ratio of these two compounds (C_{29}/C_{31}) changes marginally, with values of 0.53 and 0.56 for low- and high-carbonate samples, respectively. These values match the value of the soil sample influenced by white rot (0.56) but would also result from a hypothetical 3 : 4 mix of low-altitude and high-altitude woodland topsoils, for example. The methyl ketone distribution is unimodal peaking at C_{27}. Methyl ketones appear to correlate with *n*-alkanes with regard to concentrations (R^2 = 0.73) and chain-length distribution (R^2 = 0.94). Microbial oxidation of *n*-alkanes has widely been suggested to explain the presence of methyl ketones in soils and sediments (e.g., van Bergen et al., 1998; Cranwell et al.,

BGD
12, 12975–13039, 2015

1987; Albaigés et al., 1984) and their increase in relative concentration with sediment depth (Cranwell et al., 1987). We did not detect methyl ketones in any of our soil samples and so we assume methyl ketones to be in situ products of microbial *n*-alkane breakdown in the lake sediments.

3.3 Compound-specific isotopes

3.3.1 Carbon

Carbon isotope composition ($\delta^{13}C$) was determined for even numbered *n*-alkanoic acids ranging from C_{16}-FA to C_{30}-FA in leaf litter from sites SN, TP and GN and the topsoils from TP and GN. Furthermore, we measured $\delta^{13}C$ for C_{16} FA in *Cladophora* sp., *Potamogeton perfoliatus* and *Chara tomentosa*. The $\delta^{13}C$ values for C_{16} FA range from about −29 to −22 ‰. The C_{16} FA in *Cladophora* sp. appears the lightest (−28.7 ± 0.3 ‰) while it is slightly heavier in *Chara tomentosa* (−24.6 ± 0.2 ‰) and the heaviest in *Potamogeton perfoliatus* (−22.7 ± 0.4 ‰ ; Fig. 5). In all leaf litter samples C_{16} FA is the lightest compound, with values ranging from −36 ‰ at SN to −32 ‰ at GN. Leaf litter FAs at GN tend to be heavier while FAs at site SN are the lightest. This is particularly true for C_{16}, C_{18} and C_{22} FA. By contrast, C_{16} FA and, in particular, C_{18} FA are the heaviest compounds in the soil samples at TP and GN. Compared to the corresponding leaf litter samples, C_{16} FA and C_{18} FA are heavier by > 4 and > 3 ‰, respectively. This significant difference in the $\delta^{13}C$ values of C_{16} FA and C_{18} FA between litter and soil suggests enhanced contributions from an OM source that mainly provides isotopically heavy short-chain compounds, and heavy C_{18} FA in particular, as they are likely biosynthesized by soil OM degraders. Unlike the fractionation occurring during autotrophic CO_2 fixation, fractionation during heterotrophic OM biosynthesis is minor, leading to the view that heterotrophs such as bacterial and fungal soil OM degraders reflect the isotopic composition of their substrate (see, e.g., Boschker and Middleburg, 2002, and references therein). However, during the early stages of soil OM degradation, bacterial and fungal saprotrophs selectively consume OM compounds that are

BGD
12, 12975–13039, 2015

easy to break down, which may lead to significant differences in isotopic composition of lipids biosynthesized in situ to those in the substrate. For example, cellulose of C_3 plants is enriched in ^{13}C relative to their lipids (Hobbie and Werner, 2004). Thus, the observed shift in short-chain FA's isotopic composition between leaf litter and topsoil could be explained by selective substrate utilization by soil microbes and enhanced contributions from isotopically heavy microbial biomass. Investigating the relationship between the carbon isotopic composition of certain substrates and of short-chain FAs of 11 strains of microbes, Abraham et al. (1998) found that fungi preferentially utilized glucose from a mixed substrate to form C_{16} FA. They also found that C_{18} FA was more enriched in ^{13}C relative to C_{16} FA. Hence, it is possible that the heavy isotopic signature of both C_{16} and C_{18} FA in the topsoils and of C_{18} FA in the leaf litter results from fungal breakdown of cellulose (polysaccharide) while C_{16} FA in leaf litter still overwhelmingly derives from plant lipids. FAs of chain lengths ≥ 20 become increasingly depleted in ^{13}C with increasing chain length. Significant amounts of mid-chain C_{22} and C_{24} FAs likely derive from suberin, which may modify their isotopic composition towards slightly heavier values as small differences in the isotopic composition between root and leaf tissues have been observed (Lichtfouse et al., 1995). However, long-chain C_{26}, C_{28} and C_{30} FA probably derive solely from leaf waxes and their $\delta^{13}C$ values still show a robust decreasing trend in all investigated soil samples (average $R^2 = 0.93$), with the C_{30} FA being 0.9–2.5 ‰ lighter than C_{26} FA. Such a trend has been described previously by Lockheart et al. (1997) for long-chain *n*-alkanes (C_{27}, C_{29}, C_{31}) in leaves of *Betula ermanii*, *Quercus castaneifolia*, *Fagus japonica* and *Fagus sylvatica*, notably when the leaves were sampled in autumn. With a decrease in $\delta^{13}C$ of 2 to 4 ‰, the trend was more pronounced for *Quercus castaneifolia* and *Betula ermanii* than in *Fagus japonica* (2 ‰ change for C_{31} *n*-alkane, only). The C_{27} *n*-alkane of *Fagus sylvatica*, the species present in the high-altitude forests of the Ohrid Basin, showed a decrease of about 1 ‰ between May and October. The seasonal trend results from replenishment of leaf waxes over the course of the growing season during which both the isotopic composition of the substrate used for leaf wax biosynthesis and of the leaf wax itself

BGD
12, 12975–13039, 2015

are changing (Lockheart et al., 1997 and references therein). Finally, odd-numbered FAs are depleted in ^{13}C relative to the even-numbered FAs in the soil samples (Fig. 6), with $\delta^{13}C$ values for C_{25}, C_{27} and C_{29} FA that are lower by 0.5 ‰, on average and up to 1.1 ‰ for C_{25} FA in the high-altitude soil, for example. This difference results from the elongation of FAs following the acetyl-coenzyme A (acetyl-CoA) pathway and the fact that the methyl and carboxyl carbon atoms in acetyl-CoA have a distinctly different isotopic composition (Melzer and Schmidt, 1987; van der Meer et al., 2001). Although these patterns should also be reflected in the isotopic composition of the leaf litter lipids, we do not have enough data for the long-chain FAs from litter samples to confirm this.

3.3.2 Hydrogen

Hydrogen isotope composition was determined for even numbered FAs ranging from C_{16} to C_{32} FA in topsoils from SN, TP and GN, in leaf litter from sites SN, GN and in samples of *Potamogeton perfoliatus*, *Chara tomentosa* and *Phragmites* roots and leaves. The $\delta^{2}H$ values range from −204 ‰ for C_{16} FA in *Phragmites* roots to −119 ‰ for C_{18} FA in leaf litter from site SN (Fig. 6). On average, lipids from leaf litter and soils from all terrestrial sites are heavier (−161 ± 17 ‰) than lipids from macrophytes (−193 ± 17 ‰) by about 30 ‰, with the exception of lipids from *Phragmites* leaves that show a "terrestrial" value of −160 ± 12 ‰. The large overall range within the terrestrial lipids is mainly due to the samples from site SN, with the leaf litter being particularly heavy (−135 ± 13 ‰). This likely results from the fact that some plants contributing leaves to the litter layer utilize water vapour from year-round evaporation and condensation over the ponds of the St. Naum springs, as opposed to seasonal uptake of precipitation or soil water at the other sites. The spring water is enriched in ^{2}H relative to the local meteoric water (Matzinger et al., 2006), with very little variation year-round (Jordanoska et al., 2010), and the SN sampling site is placed in a morphologically sheltered area just a few meters above the spring-fed ponds. As the springs are active year-round delivering up to 7500 L s^{-1} with a constant temperature of 10–12 °C they create a microclimate that is cooler and more humid in the summer compared

BGD
12, 12975–13039, 2015

to the surroundings, with mist frequently forming over the ponds. This microclimate is also responsible for the specific flora occurring around the St. Naum springs (Matevski et al., 2011). Even though soil evapotranspiration rates at sites TP and GN are certainly higher than in the surroundings of the St Naum spring, it appears that the vegetation at these sites utilizes water depleted in ^{2}H compared to the main water source for the vegetation at SN. While higher evaporation rates should increase the amount of the heavy isotope in the soil water, other factors such as seasonal variability of δ^2H in precipitation presumably outweigh this fractionation process leading to the overall lighter isotope composition of plant lipids at sites TP and GN. Without monitoring of precipitation and soil water isotopic composition, we cannot fully explain these observations.

Lipid δ^2H values in soils and litter from sites TP and GN are lower and show a smaller range (-168 ± 10 ‰) compared to site SN (-142 ± 17 ‰). The heaviest compound is C_{18} FA in the TP soil samples while C_{16} FA is the lightest compound (-192 ± 10 ‰) in all soil and litter samples. Short-chain compounds are likely to derive from mixed terrestrial sources, i.e. leaf waxes as well as fungal and/or bacterial biomass. This may explain both the lighter value of C_{16} FA and the heavy C_{18} FA in the TP samples depending whether the organism takes in water directly from precipitation or water that is enriched in ^{2}H after soil evapotranspiration. In the soil from site SN, $C_{18:1}$ FA and C_{16} FA also show significantly lighter values of -177 ± 0.4 and -170 ± 2 ‰, respectively, compared to the other compounds ($C_{18:2}$ FA, C_{18}–C_{28} FA: -143 ± 13 ‰, on average) again suggesting their biosynthesis involves water derived from different sources. At site GN, on the other hand, long-chain C_{26} and C_{30} FA are the lightest compounds (-184 ± 8 and -184 ± 1 ‰, respectively), which may arise through uptake of deuterium-depleted precipitation at higher altitude.

4 Implications for proxy records

The principle behind paleoenvironmental reconstructions using organic-geochemical proxies is that OM fluxes from aquatic and terrestrial sources within the catchment

BGD
12, 12975–13039, 2015

of a given sedimentary archive change in response to changes in regional or global climate. The main purpose of this study is to characterize the organic geochemical composition of potential sources of OM buried in sediments of Lake Ohrid in order to improve the interpretation of organic geochemical proxy data in reconstructions of hydrology-controlled environmental change in the Ohrid Basin. Our initial data set provides significant insight towards an improved interpretation of changes in elemental (TOC/TN) and biomarker composition and compound-specific isotope data ($\delta^{13}C$, $\delta^{2}H$).

4.1 Assessing aquatic and terrestrial OM supply

4.1.1 Elemental composition of aquatic and terrestrial OM

TOC/TN ratios of bulk sediment are often used for assessments of aquatic and terrestrial contributions, with two values frequently applied in simple 2-endmember models: the Redfield Ratio of 6.6 for the aquatic/algal end member and the value of 20 for the terrestrial end-member (see, e.g., Meyers, 1994). As such, this approach appears of limited value in case of the Lz1120 sediments since there are at least two major terrestrial OM pools present in the Ohrid Basin with different TOC/TN signatures: plant matter/litter and soils, both of which can easily be mobilized at different rates under specific circumstances. Furthermore, macrophytes have intermediate TOC/TN ratios of 15 ± 2.4 and produce a significant amount of biomass in the littoral, intercepting nutrient supply from terrestrial run-off and directly tapping into the sedimentary nutrient pool. For example, *Potamogeton perfoliatus* L. produces a biomass of $2747 \times 10^{6}\,g\,y^{-1}$ (Talevska, 2006), while the stock of charophytes in Lake Ohrid is estimated at $10\,500 \times 10^{6}\,g$ (Trajanovska et al., 2012). Lake Ohrid is oligotrophic and the biomass from the epilimnion may well be the smallest source of sedimentary OM. A maximum phytoplankton biomass of $131\,mg\,m^{-3}$ in spring 2001 (Petrova et al., 2008) leads us to estimate a peak phytoplankton biomass in the upper 50 m of the water column of $2300 \times 10^{6}\,g$ for the spring season (calculated for lake surface area of $358\,km^{2}$),

BGD
12, 12975–13039, 2015

which is comparable to the annual production of *Potamogeton perfoliatus* L. and a quarter of the standing stock of charophytes. This OM nevertheless represents high-value food for the lake's heterotrophic consumers and is likely largely remineralised in the water column.

Straightforward interpretation of the Lz1120 TOC/TN record based on the conventional two end members therefore is not possible, but the variability of the TOC/TN record does provide valuable information on changes in OM sources in the given paleoenvironmental context. Before 8.3 ka, the estimated TOC/N_{org} ratio is 13.6 (see Sect. 3.1.3). This is higher than the value of Terra Rossa (11.4 ± 0.8), within the range of macrophytes (15 ± 2.4), and may result from any mix of these with leaf litter, topsoils and a small amount of algal material. Still, the majority of the nitrogen appears to be organic and to vary with organic carbon supply. After 8.3 ka, by contrast, TOC/TN ratios are very low, with a value of 7 at 8.05 ka close to the Redfield ratio, suggesting that the majority of the sedimentary OM always is of algal origin. This, however, is not supported by the lipid biomarkers, which are dominated by terrestrially-derived compounds throughout this period. An alternative explanation for the very low TOC/TN ratios in the Lz1120 sediments after 8.3 ka other than algal matter would be elevated amounts of inorganic nitrogen (N_{in}), for which there is some evidence (see also Sect. 3.1.3). Within the terrestrial biome, the highest proportions of N_{in} are likely to be found in the clay fraction of mineral soils. This is due to the fact that ammonium (NH_4^+), in particular, can firmly bind to clay minerals and strongly influence the soil TN pool (e.g., Elmacıet al., 2002; Kothawala and Moore, 2009; Nieder et al., 2011). The low TOC/TN value for Terra Rossa is likely due to enhanced NH_4^+ levels. Soils developing from former lake sediment during lake level low stands are also likely to be charged with NH_4^+, in particular. It has frequently been reported that the fine fraction of mineral soils contains substantially higher amounts of ammonium than the coarser soil fractions (see Nieder et al., 2011 and references therein). Size fractionation during transport of eroded mineral soil may therefore result in the deposition of clay-rich material with TOC/TN ratios that are lower than those determined for the bulk soils in situ. Hence, the low TOC/TN

BGD
12, 12975–13039, 2015

ratios in Lz1120 sediments after 8.3 ka probably result from enhanced supply of clay-bound ammonium following mineral soil erosion rather than algal OM.

4.1.2 Aquatic and terrestrial biomarkers

Nearly all of the biomarkers preserved in the sediments can be ascribed to terrestrial OM, or have a non-specific source. The exception is dinosterol (from dinoflagellates), but this is a very minor component of the total lipid extracts and we consider it not to be a robust quantitative proxy for lake-derived OM.

The amount of lipids relative to the total OM of individual sources is likely to vary with environmental conditions. Thus, without knowledge on how representative individual biomarkers are for the size of the OM pool they derive from under specific hydrological conditions, assessments of relative contributions remain speculative unless they are backed up by other proxy data (e.g., elemental data, petrology, bulk isotopes).

4.1.3 Carbon and hydrogen stable isotopes of C_{16} FA from aquatic and terrestrial OM

Interpreting compound-specific isotopic data ($\delta^{13}C$, $\delta^{2}H$), for example using the C_{16} FA, which is present in all terrestrial and lacustrine samples is not straightforward. Hence, in soil and leaf litter samples there is a range of > 7 ‰ (-29 to -36 ‰) in $\delta^{13}C$. Since both are likely sources of OM to the lake, then change in sedimentary C_{16} FA $\delta^{13}C$ might simply reflect the strength of the soil vs. litter supply, rather than any change in terrestrial vs. aquatic source. A variation of > 6 ‰ in macrophyte samples adds to the uncertainties. Using a similar approach with $\delta^{2}H$ may be more fruitful as on average the difference between terrestrial and aquatic sources is ca. 30 ± 8 ‰ for the C_{16} FA. However, even within the limited number of soil and leaf litter samples analysed, there is > 40 ‰ variation in $\delta^{2}H$. Factors such as the amount of microbial biomass contributing to the terrestrial OM, variable input of emergent macrophytes (*Phragmites* leaves), or a local moisture sources (St Naum springs) all enhance overall

BGD
12, 12975–13039, 2015

variability and complexity. Developing a mixing model for aquatic vs. terrestrial OM in the sediments using $\delta^{13}C$ and $\delta^{2}H$ therefore appears challenging.

4.2 Identifying the changing composition of terrestrial OM using lipid biomarkers

As evident from the pie diagrams in Fig. 3, topsoils contain significantly higher amounts of *n*-alcohols (OHs) relative to *n*-alkanoic acids (FAs) than leaf litter. The mineral soil (Terra Rossa) contains even higher proportions of OHs, accounting for almost half of the total lipids, and very low amounts of FAs. Thus, the ratio of sedimentary *n*-alkanoic acids over *n*-alcohols (FA/OH) is indicative of shifts in the contribution from these major terrestrial sources, with higher ratios indicating higher proportions of plant litter relative to soil OM and lower ratios indicating enhanced contributions from topsoils and/or mineral soils. Since a significant amount of short-chain FAs, *n*-C_{16} FA in particular, may also derive from aquatic sources we consider the ratio of long-chain FA over long-chain OH of certain terrestrial origin (terr FA/OH) to be a more reliable measure. Notably, both ratios, FA/OH and terr FA/OH, correlate well in the sediment samples ($R^2 = 0.99$ for all samples, $R^2 = 0.95$ for high-carbonate samples) suggesting that aquatic sourced short-chain FAs are of minor importance.

The chain-length distributions in Fig. 3 also reveal another important difference between leaf litter and soils. In the near-shore oak-dominated biome, the proportion of mid-chain FAs, C_{22} and C_{24} FA in particular, is higher relative to long-chain FAs ($\geq C_{26}$) in the topsoil and in Terra Rossa than in the corresponding leaf litter. The ratio of sedimentary mid-chain C_{22} and C_{24} FAs over long-chain C_{26}, C_{28} and C_{30} FAs should therefore be sensitive to soil OM supply from the near-shore biome. Similar increases in the proportion of mid-chain FAs in soils relative to litter have also been observed in topsoils of a high-altitude beech forest in Central France (Marseille et al., 1999) and of an evergreen oak forest in Central Spain (Almendros et al., 1996). In a forest topsoil from the surroundings of Lake Suwa in Japan (Matsuda and Koyama, 1977), which represents a setting very similar to the Ohrid Basin (mid-latitude, high-altitude intra-

BGD
12, 12975–13039, 2015

mountainous lake basin with moist forest biome), FA distributions in the topsoils are very similar to that at site SN (R^2 = 0.90), providing evidence that, generally, similar natural processes operate under similar environmental conditions. The chain-length distributions of the *n*-alcohols also reveal differences between the terrestrial sources (Fig. 3), which are most pronounced between high-altitude and low-altitude sources when expressed, for example, as the average chain length (ACL) of C_{24} to C_{28} OHs ($ACL_{24–28}$). The amounts of *n*-alcohols are significantly higher in soils than in leaf litter. Changes in $ACL_{24–28}$ in the sediments therefore potentially indicate variable contributions of soil OM from high-altitude beech-dominated or low-altitude oak-dominated biome types. *n*-Alkane distributions, finally, allow for a clear distinction between C_{27}-dominated and C_{29}-dominated leaf litter from the high and low-altitude forests, respectively. In the soils, the input of C_{31} *n*-alkane significantly increases (Fig. 3) and probably reflects incorporation of lipids from the grassy undergrowth or from an earlier, more open type of vegetation. In the sediments, the amounts of *n*-C_{27} alkane are always significantly lower than the *n*-C_{29} alkane, suggesting that contribution from the high-altitude biome is minor. In fact, the *n*-alkane distribution of a hypothetical 1 : 1 mix of *n*-alkanes from low-altitude topsoil and Terra Rossa correlates very well with the average sedimentary *n*-alkane distribution (R^2 = 0.95). Similarly, the high-proportion of the *n*-C_{31} alkane indicates that inputs of leaf litter from beech or oak are minor relative to soil OM. Two observations suggest that the popular application of certain *n*-alkane ratios (*n*-C_{27} or *n*-C_{29} relative to *n*-C_{31}) as proxies for the development of the vegetation (mainly for trees vs. grass/shrubs; e.g., Schwark et al., 2002; Zhang et al., 2006; Leider et al., 2013) is compromised in the Ohrid Basin: (a) the bimodal *n*-alkane distribution in high-altitude topsoil and (b) the similarity of the distributions in soils and sediments that distinctly differ from the pronounced unimodal leaf litter distributions. The ambiguity of proxies based on these ratios in the Ohrid Basin is highlighted by the fact that, for example, the C_{29}/C_{31} *n*-alkane ratio in both high-carbonate samples (warmer, more humid climate) and low-carbonate samples (cooler, more arid climate) are very simi-

BGD
12, 12975–13039, 2015

lar, 0.56 and 0.53, respectively, even though the biome certainly changed significantly through the pronounced climatic fluctuation of the 8.2 ka event.

MDS shows separation of sample types, namely soils, leaf litter, macrophytes, lake POM and sediments, which 1-way ANOSIM shows to be significantly different. The "weakest" differences are between soil and lake sediment ($R = 0.463$, $P = 1\,\%$) and soil and leaf litter ($R = 0.487$, $P = 5.4\,\%$), the latter not being significantly different. This is also evident in the MDS plot (Fig. 7), which shows that the soils are close in Euclidian space to the sediments and implies that the composition of the sediments is dominated by soil-derived lipids. If the analysis is restricted to the lake sediments only, then again, there is a significant difference between the low carbonate and other sediments ($R = 0.734$, $P = 0.6\,\%$). This is particularly clear for the sediments that are interpreted to reflect the 8.2 ka event (Figs. 2 and 9), which are on the other hand, much closer in MDS space to the single sample of Terra Rossa soil.

4.3 Application of new proxies across the 8.2 ka climate event

Figure 8 compares the elemental records across the 8.2 ka event to biomarker proxies that are based on our geochemical fingerprinting of modern OM sources. The carbonate record shows two pronounced minima in response to changes in temperature and hydrology (Wagner et al., 2008) that likely reflect the Northern Hemisphere climate development controlled by two major phases of freshwater release into the North Atlantic (Lajeunesse and St-Onge, 2008; Roy et al., 2011). In the following, we refer to the timing of these minima as Phase 1 and Phase 2 according to their chronological succession. While the carbonate record is closely linked to climate forcing, the proxies that incorporate an organic component, i.e. TOC, TOC/TN, the concentration of total lipids and the biomarker ratios, are controlled by the response of the biome and associated changes in OM fluxes to the lake sediments.

Between 8.7 and 8.35 ka, TOC and TOC/TN values are relatively high as is the terr FA/OH ratio. These data are consistent with high- and low-altitude topsoils (terr FA/OH 0.7 and 0.9, respectively) and leaf litter (terr FA/OH 0.5 and 0.7, respectively) being

BGD
12, 12975–13039, 2015

the main sources of sedimentary OM between 8.7 and 8.35 ka, while the contribution from Terra Rossa (terr FA/OH 0.1) is minimal. Notably, the concentration of the total lipids steadily decreases from 8.7 ka onwards, indicating a decline in the supply of lipid-rich material and a gradual change in the make-up of the terrestrial biome. A similar trend can be seen in the $ACL_{22–26}$ FA between 8.7 and 8.5 ka, but not in $ACL_{24–28}$ OH indicating an early change in the lipid sources. This subtle shift can also be discerned in the TOC/TN ratios. While the ultimate driver behind these early trends is certainly a slowly changing regional climate, more immediate forcing factors may have included:

1. A slowly decreasing lake level, exposing the flood plains to the south of site Lz1120 and reducing the flux of lipid-rich terrestrial OM to the lake.

2. A change in the soil moisture budget leading to increased degradation of lipids.

3. A slow decline in terrestrial productivity.

Due to its tectonic origin, the Ohrid Basin is characterized by a pronounced terraced morphology, particularly at its northern and southern ends where today's agricultural plains were once marsh land and/or lake floor. As a result, lake level change can introduce a threshold-type control of biome characteristics and, thus, cause abrupt changes in material fluxes within the catchment of site Lz1120.

A major change occurred shortly after 8.35 ka, with the onset of Phase 1, when values for carbonate, TOC and TOC/TN dropped sharply, indicating a substantial change in the deposition of OM quantity and composition. While the carbonate record suggests a short "recovery" followed by another, slightly prolonged but less pronounced minimum during Phase 2, the records of TOC and TOC/TN reveal that the non-carbonate sediment delivered during Phases 1 and 2 contained bulk OM of significantly different quantity and composition. During Phase 1, an increased supply of non-carbonate material apparently contributed little OM and diluted both carbonate and TOC while the sedimentary OM shows low TOC/TN ratios. During Phase 2, by contrast, TOC/TN ratios were higher and TOC was either less diluted and/or the non-carbonate material

BGD
12, 12975–13039, 2015

supplied to the lake contained higher amounts of OM. This difference in OM composition between Phases 1 and 2 is confirmed by the composition of the total lipid extracts that generally contain high proportions of both long-chain terrestrial *n*-alkanoic acids and *n*-alcohols, but show a substantial drop in the terr FA/OH ratio in Phase 2, only. Conversely, the average chain length of *n*-alcohols ($ACL_{24–28}$ OH) does not show any significant change except for a minimum in Phase 1. The ratio of largely suberin-derived mid-chain over plant wax-derived long-chain *n*-alkanoic acids (m-FA/l-FA), on the other hand, shows maxima in both phases. In order to explain these patterns, variable contributions from the terrestrial OM pools, low- and high-altitude litter and topsoil as well as mineral soil, need to be considered. For Phase 1, higher values of m-FA/l-FA and a lower $ACL_{22–26}$ FA and $ACL_{24–28}$ OH are consistent with the lipid fingerprint of a low-altitude topsoil. However, the shifts in the elemental data require substantial supply of a material with very low amounts of carbonate and TOC, lower TOC/TN ratios and lowest lipid concentrations. An enhanced supply of Terra Rossa type soil would explain this pattern, but the terrigenous FA/OH ratio that clearly distinguishes Terra Rossa from all other OM sources remains high. An alternative OM source with low TOC/TN ratios and TOC values could be former lake sediment. This would have been deposited in the shallow areas to the south and southwest of Lz1120 at lake level high-stands and would have been spiked with suberin-derived mid-chain FA and OH during a slowly falling lake level and the development of marshy vegetation while the high groundwater table would have dissolved the carbonate. In fact, the lipid composition of the sample from 8.29 ka (Phase 1), despite showing different values for the m-FA/l-FA ratio and $ACL_{22–26}$ FA, overall does not significantly differ from the total lipid composition of samples with high carbonate contents (Fig. 7). Silty agricultural soils of brown-grey color that appear most likely to have developed from former lake sediment can be found, for example, in the fields to the south of Pogradec, with variable amounts of fine sand incorporated into the clayey silt matrix deriving from former beach lines. The shift in the geochemical records in Phase 1 may thus be explained by enhanced erosion of material from the exposed plains, combined with some contribution from sur-

BGD
12, 12975–13039, 2015

rounding low-altitude topsoils. This also implies that the lake level must have dropped to roughly the modern level or below at the time. Unfortunately, we do not have the geochemical fingerprint for the marshy element of the biome to verify this hypothesis. By contrast, while an even more pronounced peak in the m-FA/l-FA ratio and a minimum in $ACL_{22–26}$ FA again suggest increased supply of suberin-derived lipids, the significant drop in the terrigenous FA/OH ratio observed in Phase 2 clearly suggests substantial contributions from Terra Rossa. In contrast to Phase 1, the values for $ACL_{22–26}$ FA and $ACL_{24–28}$ OH in Phase 2 strongly diverge, which also agrees with supply of lipids mainly from Terra Rossa as the latter has significantly higher proportions of C_{28} OH compared to the low-altitude topsoils (Fig. 3). MDS analysis confirms the assumption of significant contribution from Terra Rossa as the samples from 8.17 and 8.11 ka plot closest to the Terra Rossa sample (Fig. 7).

Mineral soils as the main source of sedimentary lipids and little contribution from topsoils or of terrestrial vegetation suggests that the latter were both diminished, leaving the deeper soil layers vulnerable to erosion. A depleted topsoil pool and, possibly, a vegetation cover that had not yet fully recovered from a period of at least seasonally increased aridity would also explain why the samples from 8.23 ka (separating Phases 1 and 2) and from 8.05 ka show TOC values that appear low relative to their carbonate contents, with these two proxies otherwise correlating closely (R^2 = 0.88 between 8.8 and 8.0 ka, without samples from 8.05 and 8.23 ka). By contrast, carbonate supply from primary production and carbonate precipitation would have increased rapidly under warmer and more humid conditions and with increased nutrient supply.

Finally, the composition of *n*-alkanes in Fig. 8 apparently follows the concentration of the total lipids, with higher proportions of supposedly grass-derived *n*-C_{31} alkane relative to the tree-derived *n*-C_{27} and *n*-C_{29} alkanes coinciding with lower concentrations of sedimentary lipids. The supply of Terra Rossa may contribute to this pattern, as it contains very low amounts of lipids and significantly higher proportions of the C_{31} alkane. Considering the fact that the incorporation of lipids into the mineral soil is likely lagging the development of the overlying topsoil and vegetation makes the application of

BGD
12, 12975–13039, 2015

n-alkane distributions for vegetation reconstructions in the Ohrid Basin challenging. By contrast, biomarker proxies based on chain-length distributions and proportions of the major lipid compound classes, FA and OH, appear to follow a pattern that is consistent with the climatic development and likely biome and lake level changes.

Since Lake Ohrid appears to have been an oligotrophic ecosystem for most of its history, it is not surprising that soil OM is the major source of the sedimentary lipids. Our lipid-based proxies suggest that soil OM supply was relatively enhanced during the 8.2 ka event in response to a dryer and cooler climate and the associated recession of terrestrial vegetation. This contradicts the conclusions of Lacey et al. (2014) who assume a reduction in primary productivity and an even more profound reduction in the contribution of soil-derived OM for the period between 8.5 and 8.0 ka, based on their interpretation of proxy data from bulk organic carbon isotope measurements and Rock-Eval pyrolysis of sediments from the western part of Lake Ohrid. The authors postulate lower soil-OM contributions on the basis of heavier bulk carbon isotopes and higher values of the oxygen index (OI) from Rock-Eval pyrolysis. However, soil OM is frequently characterized by the same pattern, i.e. bulk carbon isotope ratios that are heavier by 1–3 ‰ compared to the original vegetation (Lichtfouse et al., 1995; Ehleringer et al., 2000 and references therein) and higher OI values (Disnar et al., 2003). This results from initial OM degradation in the soils rather than in the water column as assumed by Lacey et al. (2014). We therefore suggest that the data reported by Lacey et al. (2014) actually supports our conclusion of relatively increased amounts of soil-derived OM in the Lake Ohrid sediments between about 8.5 and 8.0 ka.

5 Summary and conclusions

Lake Ohrid is an outstanding sedimentary archive of SE European continental climate change, recording environmental changes in the Ohrid Basin continuously for at least 1.2 million years. OM buried in Lake Ohrid sediments can deliver information on the response of the ecosystem to climatically controlled changes in hydrology. In order to

BGD
12, 12975–13039, 2015

optimize the reconstruction of environmental changes we carried out the first organic geochemical survey of potential sources of sedimentary OM in the Ohrid Basin.

We determined the organic geochemical fingerprints of leaf litter, topsoil, mineral soil, macrophytes and filtrates of suspended and slow-sinking particles from the Ohrid water column. Comparison with the TLE composition of Early Holocene sediments from site Lz1120 in the southeast of Lake Ohrid reveals that little of the sedimentary lipids appear to derive from aquatic OM sources such as macrophytes of phytoplankton. Labile compounds including MUFAs and PUFAs, accounting for a third of the polar lipids in water filtrates and up to half of the total lipids in macrophytes, are not preserved in the sediments, while the dominant saturated fatty acid in these samples, the *n*-hexadecanoic acid, is not source specific. By contrast, the majority of the sedimentary lipids are from land sources. Apart from long-chain ($> C_{24}$) *n*-alkanoic acids (FAs) and *n*-alcohols (OHs) that derive from cuticular waxes, mid-chain C_{22} and C_{24} FAs, ω-hydroxy FAs (ω-OH-FAs) and OHs most likely are from suberin, a bio-polyester forming protective tissue mainly in roots but also barks and bundle sheaths of grasses. The C_{22} and C_{24} ω-OH-FAs appear to be particularly reliable indicators for soil-derived OM as they were present in all topsoil samples but largely absent in leaf litter, macrophytes and water filtrates. With proportions of ω-OH-FA showing an almost identical range in soils and sediments of about $4 \pm 2\,\%_{\text{lipids}}$ on average, each, we conclude that the majority of the extracted lipids originates from soil OM with considerable inputs from root material. This is supported by the generally high amounts of suberin-derived mid-chain FA and OH. Terra Rossa, the most abundant type of mineral soil in the East and South of the Ohrid Basin, contains little organic carbon compared to the topsoils (1 vs. 8–11 %) and, accordingly, only small amounts of lipids. Notably, the terr FA/OH ratio is significantly lower in Terra Rossa, making the ratio of these compound classes a useful indicator for substantial soil erosion. The lipid composition of the sediments is closest to the composition of topsoils and, in some cases, likely represents a mixture of topsoil and mineral soil lipids.

BGD
12, 12975–13039, 2015

We tested a set of new proxies based on our improved end-member characterizations for a section of sediment core Lz1120 that includes the prominent 8.2 ka event, a 400 to 500 year episode of cold and dry climate in the North Atlantic realm affecting much of the Northern Hemisphere, including SE Europe. Both the carbonate record and the biomarker proxies highlight two distinct phases of the 8.2 ka event affecting the ecosystems of the Ohrid Basin. Changing proportions of suberin-derived mid-chain compounds relative to cuticular long-chain compounds as expressed in ratios (m-FA/l-FA) or average chain lengths ($ACL_{C22–26}$ FA, $ACL_{C24–28}$ OH) combined with the proportion of terrestrial *n*-alkanoic acids over *n*-alcohols (terr FA/OH) indicating contributions from mineral soil (Terra Rossa) also reveal significant differences between the two phases in with regard to lipid fluxes from the major OM sources. Accordingly, Phase 1 (~ 8.3 ka) is characterized by relatively enhanced contribution of lipids from topsoils while Phase 2 (8.2–8.05 ka) shows clear evidence for a substantial proportion of lipids derived from mineral soil, suggesting that the topsoil OM pool had already been depleted in Phase 1, or that soil erosion was more severe as the deeper soils were less protected by the modified vegetation cover. Notably, the biomarker proxies show a consistent trend of biome modification starting early from 8.65 ka onwards that is consistent with a similar trend in carbonate, TOC and TOC/TN and occurs well before the substantial change at the onset of Phase 1. These trends result from a continuous change in the hydrology of the Ohrid Basin and underline the sensitivity of the biomarker approach.

Overall, it appears that soil-derived lipids have the greatest potential to be preserved in the sedimentary archive of the Ohrid Basin. However, the extent as to which terrigenous and aquatic biomarkers are representative of the terrestrial and aquatic OM pools still is a matter of uncertainty. Multi-proxy approaches combining lipid analyses with, for example, bulk carbon and hydrogen stable isotope data, pyrolysis GC-MS analyses or Rock-Eval analyses of both OM sources and sediments may help resolve this issue. Further improvements of biomarker-based biome reconstructions may be achieved by completing the geochemical characterization of elements of the Ohrid

BGD
12, 12975–13039, 2015

biome that are currently missing including as grasses, marshland soils and soils developing on the ultrabasic rocks along the western shores. However, our first survey of major OM sources in the Ohrid Basin demonstrates that organic-geochemical fingerprinting and the development of proxies adjusted to the local OM inventory can lead to an improved understanding of terrestrial biome dynamics and OM fluxes towards the lake sediments, in particular, when short-distance OM transport in a heterogeneous and variable catchment significantly increase complexity. When applied to the sedimentary record of a well-known climate fluctuation, the 8.2 ka event, the adjusted proxies demonstrably improve the interpretation of bulk-proxy data such as TOC and TOC/TN.

The Supplement related to this article is available online at doi:10.5194/bgd-12-12975-2015-supplement.

Acknowledgements. We are grateful to D. Kurti (Pogradec) for logistical support during macrophyte sampling, O. Cara (Durrës) and B. Muceku (Tirana) for support during soil sampling and treatment and B. Wagner and A. Franke (Cologne) for providing the sediment samples. Finally, we thank A. Thompson, S. Blackbird (Liverpool) and P. Donohoe (Newcastle) for support in the laboratories. The study was funded by the Leverhulme Trust (grant F/00 025/AU).

References

Abraham, W. R., Hesse, C., and Pelz, O.: Ratios of carbon isotopes in microbial lipids as an indicator of substrate usage, Appl. Environ. Microb., 64, 4202–4209, 1998.

Albaigés, J., Algaba, J., and Grimalt, J.: Extractable and bound neutral lipids in some lacustrine sediments, Org. Geochem., 6, 223–236, 1984.

Almendros, G., Sanz, J., and Velasco, F.: Signatures of lipid assemblages in soils under continental Mediterranean forests, Eur. J. Soil Sci., 47, 183–196, 1996.

BGD
12, 12975–13039, 2015

Apolinarska, K., Pełechaty, M., and Pukacz, A.: $CaCO_3$ sedimentation by modern charophytes (Characeae): can calcified remains and carbonate $\delta^{13}C$ and $\delta^{18}O$ record the ecological state of lakes? – a review, Stud. Lim. Tel., 5, 55–66, 2011.

Barber, D. C., Dyke, A., Hillaire-Marcel, C., Jennings, A. E., Andrews, J. T., Kerwin, M. W., Bilodeau, G., McNeely, R., Southon, J., Morehead, M. D., and Gagnon, J.-M.: Forcing of the cold event of 8,200 years ago by catastrophic drainage of Laurentide lakes, Nature, 400, 344–348, 1999.

Birks, H. H. and Birks, H. J. B.: Multi-proxy studies in palaeolimnology, Veg. Hist. Archaeobot., 15, 235–251, 2006.

Boschker, H. T. S. and Middelburg, J. J.: Stable isotopes and biomarkers in Microbiol Ecology, FEMS Microbiol. Ecol., 40, 85–95, 2002.

Bumrela, S. B. and Naik, S. R.: Identification of β-carotene and β-sitosterol in methanolic extract of *Dipteracanthus patulus* (Jacq) nees and their role in antimicrobial and antioxidant activity, Int. J. Phytomed., 3, 204–215, 2011.

Chevolleau, S., Mallet, J. F., Debal, A., and Ucciani, E.: Antioxidant activity of Mediterranean plant leaves: occurrence and antioxidative importance of α-tocopherol, J. Am. Oil Chem. Soc., 70, 807–809, 1993.

Costantini, E. A. C., Barbetti, R., Fantappiè, M., L'Abate, G. L., Lorenzetti, R., and Magini, S.: Pedodiversity, in: The Soils of Italy, edited by: Costantini, E. A. C. and Dazzi, C., World Soils Book Series, Springer, Dordrecht, 105–178, doi:10.1007/978-94-007-5642-7_6, 2013.

Cranwell, P. A., Eglinton, G., and Robinson, N.: Lipids of aquatic organisms as potential contributors to lacustrine sediments – II, Org. Geochem., 11, 513–527, 1987.

Disnar, J. R., Guillet, B., Keravis, D., Di-Giovanni, C., and Sebag, D.: Soil organic matter (SOM) characterization by Rock-Eval pyrolysis: scope and limitations, Org. Geochem., 34, 327–343, 2003.

Douglas, P. M. J., Pagani, M., Eglinton, T. I., Brenner, M., Hodell, D. A., Curtis, J. H., Ma, K., and Breckenridge, A.: Pre-aged plant waxes in tropical lake sediments and their influence on the chronology of molecular paleoclimate proxy records, Geochim. Cosmochim. Ac., 346–364, doi:10.1016/j.gca.2014.06.030, 2014.

Ehleringer, J. R., Buchmann, N., and Flanagan, L. B.: Carbon isotope ratios in belowground carbon cycle processes, Ecol. Appl., 10, 412–422, 2000.

Ellison, C. R. W., Chapman, M. R., and Hall, I. R.: Surface and deep ocean interactions during the cold climate event 8200 years ago, Science, 312, 1929–1932, 2006.

BGD
12, 12975–13039, 2015

Elmacı, Ö. L., Seçer, M., Erdemir, O., and Iqbal, N.: Ammonium fixation properties of some arable soils from the Aegean region of Turkey, Eur. J. Agron., 17, 199–208, 2002.
Ficken, K. J., Li, B., Swain, D. L., and Eglinton, G.: An *n*-alkane proxy for the sedimentary input of submerged/floating freshwater aquatic macrophytes, Org. Geochem., 31, 745–749, 2000.
Fontanel, D., Kargol, M., Gueiffier, A., and Viel, C.: Triterpene alcohols and fatty acids in lipids and nonsaponifiable matter of *Lapsana communis* L. subspecies *communis* (Asteraceae), J. Am. Oil Chem. Soc., 75, 1457–1459, 1998.
Ghandi, S. R. and Weete, J. D.: Production of the polyunsaturated fatty acids arachidonic acid and eicosapentaenoic acid by the fungus *Pythium ultimum*, J. Gen. Microbiol., 137, 1825–1830, 1991.
Graça, J. and Santos, S.: Suberin: a biopolyester of plants' skin, Macromol. Biosci., 7, 128–135, 2007.
Grootes, P. M., Stuiver, M., White, J. W. C., Johnsen, S., and Jouzel, J.: Comparison of oxygen isotope records from the GISP2 and GRIP Greenland ice cores, Nature, 366, 552–554, 1993.
Hobbie, E. A. and Werner, R. A.: Intramolecular, compound-specific, and bulk carbon isotope patterns in C_3 and C_4 plants: a review and synthesis, New Phytol., 161, 371–385, 2004.
Holtvoeth, J., Vogel, H., Wagner, B., and Wolff, G. A.: Lipid biomarkers in Holocene and glacial sediments from ancient Lake Ohrid (Macedonia, Albania), Biogeosciences, 7, 3473–3489, doi:10.5194/bg-7-3473-2010, 2010.
Jaffé, R., Mead, R., Hernandez, M. E., Peralba, M. C., and DiGuida, O. A.: Origin and transport of sedimentary organic matter in two subtropical estuaries: a comparative, biomarker-based study, Org. Geochem., 32, 507–526, 2001.
Jordanoska, B., Kunz, M. J., Stafilov, T., and Wüest, A.: Temporal variability of physico-chemical properties of St. Naum karst springs feeding Lake Ohrid, J. Environ. Prot. Ecol., 13, 3–11, 2010.
Kiriakoulakis, K., Marshall, J. D., and Wolff, G. A.: Biomarkers in a Lower Jurassic concretion from Dorset (UK), J. Geol. Soc. London, 157, 207–220, 2000.
Kothawala, D. N. and Moore, T. R.: Adsorption of dissolved nitrogen by forest mineral soils, Can. J. Forest Res., 39, 2381–2390, 2009.
Królikowska, J.: Eutrophication processes in a shallow, macrophyte-dominated lake – species differentiation, biomass and the distribution of submerged macrophytes in Lake Łuknajno (Poland), Hydrobiologia, 342/343, 411–416, 1997.

BGD
12, 12975–13039, 2015

Lacey, J. H., Francke, A., Leng, M. J., Vane, C. H., and Wagner, B.: A high resolution Late Glacial to Holocene record of environmental change in the Mediterranean from Lake Ohrid (Macedonia/Albania), Int. J. Earth Sci., 103, in press, doi:10.1007/s00531-014-1033-6, 2014.

Lajeunesse, P. and St-Onge, G.: The subglacial origin of the Lake Agassiz–Ojibway final outburst flood, Nat. Geosci., 1, 184–188, 2008.

Leider, A., Hinrichs, K.-U., Schefuß, E., and Versteegh, G. J. M.: Distribution and stable isotopes of plant wax derived *n*-alkanes in lacustrine, fluvial and marine surface sediments along an Eastern Italian transect and their potential to reconstruct the hydrological cycle, Geochim. Cosmochim. Ac., 117, 16–32, 2013.

Leng, M. J., Baneschi, I., Zanchetta, G., Jex, C. N., Wagner, B., and Vogel, H.: Late Quaternary palaeoenvironmental reconstruction from Lakes Ohrid and Prespa (Macedonia/Albania border) using stable isotopes, Biogeosciences, 7, 3109–3122, doi:10.5194/bg-7-3109-2010, 2010.

Lichtfouse, É., Dou, S., Girardin, C., Grably, M., Balesdent, J., Behar, F., and Vandenbroucke, M.: Unexpected ^{13}C-enrichment of organic components from wheat crop soils: evidence for the in situ origin of soil organic matter, Org. Geochem., 23, 865–868, 1995.

Lockheart, M. J., van Bergen, P. F., and Evershed, R. P.: Variations in the stable carbon isotope compositions of individual lipids from the leaves of modern angiosperms: implications for the study of higher land plant-derived sedimentary organic matter, Org. Geochem., 26, 137–153, 1997.

Marseille, F., Disnar, J. R., Guillet, B., and Noack, Y.: *n*-Alkanes and free fatty acids in humus and A1 horizons of soils under beech, spruce and grass in the Massif-Central (Mont-Lozère), France, Eur. J. Soil Sci., 50, 433–441, 1999.

Matevski, V., Čarni, A., Avramoski, O., Juvan, N., Kostadinovski, M., Košir, P., Marinšek, A., Paušič, A., and Šile, U.: Forest Vegetation of the Galičica Mountain Range in Macedonia, Založba ZRC, Ljubljana, 200 pp., ISBN 978-961-254-313-6, 2011.

Matsuda, H. and Koyama, T.: Early diagenesis of fatty acids in lacustrine sediments – II. A statistical approach to changes in fatty acid composition from recent sediments and some source materials, Geochim. Cosmochim. Ac., 41, 1825–1834, 1977.

Matzinger, A., Jordanoski, M., Veljanoska-Sarafiloska, E., Sturm, M., Müller, B., and Wüest, A.: Is Lake Prespa jeopardizing the ecosystem of ancient Lake Ohrid?, Hydrobiologia, 553, 89–109, doi:10.1007/s10750-005-6427-9, 2006.

BGD
12, 12975–13039, 2015

Matzinger, A., Schmid, M., Veljanoska-Sarafiloska, E., Patceva, S., Guseska, D., Wagner, B., Müller, B., Sturm, M., and Wüest, A.: Eutrophication of ancient Lake Ohrid: global warming amplifies detrimental effects of increased nutrient inputs, Limnol. Oceanogr., 52, 338–353, 2007.

Matzke, K. and Riederer, M.: A comparative study into the chemical constitution of cutins and suberins from *Picea abies* (L.) Karst., *Quercus robur* L., and *Fagus sylvatica* L., Planta, 185, 233–245, 1991.

Melzer, E. and Schmidt, H.-L.: Carbon isotope effects on the pyruvate dehydrogenase reaction and their importance for relative carbon-13 depletion in lipids, J. Biol. Chem., 262, 8159–8164, 1987.

Mendez-Millan, M., Dignac, M.-F., Rumpel, C., and Derenne, S.: Can cutin and suberin biomarkers be used to trace shoot and root-derived organic matter? A molecular and isotopic approach, Biogeochemistry, 106, 23–28, 2011.

Mertz, R. A. and Brutnell, T. P.: Bundle sheath suberization in grass leaves: multiple barriers to characterization, J. Exp. Bot., 65, 3371–3380, 2014.

Meyers, P. A.: Preservation of elemental and isotopic source identification of sedimentary organic matter, Chem. Geol., 114, 289–302, 1994.

Meyers, P. A. and Lallier-Vergès, E.: Lacustrine sedimentary organic matter records of Late Quaternary paleoclimates, J. Paleolimnol., 21, 345–372, 1999.

Mikolajczak, K. L. and Smith Jr., C. R.: Pentacylic triterpenes of *Jurinea anatolic* boiss., and *Jurinea consanguinea* DC. fruit, Lipids, 2, 127–132, 1967.

Ministry of Environment and Physical Planning: Biodiversity Strategy and Action Plan for the Republic of Macedonia, Ministry of Environment and Physical Planning, Skopje, 134 pp., ISBN:9989-110-16-6, 2003.

Molina, I., Bonaventure, G., Ohlrogge, J., and Pollard, M.: The lipid polyester composition of *Arabidopsis thaliana* and *Brassica napus* seeds, Phytochemistry, 67, 2597–2610, 2006.

Muley, B. P., Khadabadi, S. S., and Banarase, N. B.: Phytochemical constituents and pharmacological activities of *Calendula officinalis* Linn (Asteraceae): a review, Trop. J. Pharm. Res., 8, 455–465, 2009.

Nair, J. J., Aremu, A. O., and Van Staden, J.: Anti-inflammatory effects of *Leucosidea sericea* (Rosaceae) and identification of the active constituents, S. Afr. J. Bot., 80, 75–76, 2012.

Nieder, R., Benbi, D. K., and Scherer, H. W.: Fixation and defixation of ammonium in soils: a review, Biol. Fert. Soils, 4, 1–14, 2011.

BGD
12, 12975–13039, 2015

Nierop, K. G. J., Naafs, D. F. W., and van Bergen, P. F.: Origin, occurrence and fate of extractable lipids in Dutch coastal dune soils along a pH gradient, Org. Geochem., 36, 555–566, 2005.
Petrova, D., Patceva, S., Mitic, V., Shtereva, G., and Gerdzhikov, D.: State of phytoplankton community in the Bulgarian and Macedonian lakes, J. Environ. Prot. Ecol., 9, 501–512, 2008.
Pollard, M., Beisson, F., Li, Y., and Ohlrogge, J. B.: Building lipid barriers: biosynthesis of cutin and suberin, Trends Plant Sci., 13, 236–246, 2008.
Reis, F. S., Ferreira, I. C. F. R., Barros, L., and Martins, A.: A comparative study of tocopherols composition and antioxidant properties of in vivo and in vitro ectomycorrhizal fungi, LWT-Food Sci. Technol., 44, 820–824, 2011.
Robinson, N., Cranwell, P. A., Eglinton, G., and Jaworsk, G. H. M.: Lipids of four species of freshwater dinoflagellates, Phytochemistry, 26, 411–421, 1987.
Roy, M., Dell'Oste, F., Veillette, J. J., de Vernal, A., Hélie, J.-F., and Parent, M.: Insights on the events surrounding the final drainage of Lake Ojibway based on James Bay stratigraphic sequences, Quaternary Sci. Rev., 30, 682–692, 2011.
Ruess, L., Schütz, K., Haubert, D., Häggblom, M. M., Kandeler, E., and Scheu, S.: Application of lipid analysis to understand trophic interactions in soil, Ecology, 86, 2075–2082, 2005.
Samuels, L., Kunst, L., and Jetter, R.: Sealing plant surfaces: cuticular wax formation by epidermal cells, Annu. Rev. Plant Biol., 59, 683–707, 2008.
Schwark, L. Zink, K., and Lechterbeck, J.: Reconstruction of postglacial to early Holocene vegetation history in terrestrial Central Europe via cuticular lipid biomarkers an pollen records from lake sediments, Geology, 30, 463–466, 2002.
Shimizu, S., Kawashima, H., Shinmen, Y., Akimoto, K., and Yamada, H.: Production of eicosapentaenoic acid by *Mortierella* fungi, J. Am. Oil Chem. Soc., 65, 1455–1459, 1988.
Soukup, A., Armstrong, W., Schreiber, L., Franke, R., and Votrubová, O.: Apoplastic barriers to radial oxygen loss and solute penetration: a chemical and functional comparison of the exodermis of two wetland species, *Phragmites australis* and *Glyceria maxima*, New Phytol., 173, 264–278, 2007.
Talevska, M.: Annual biomass and production of Red Head Grass (*Potamogeton Perfoliatus* L.) from Lake Ohrid, paper presented at the 2nd conference of the Balkan Water Observation and Information System (BALWOIS), Balwois Network, Ohrid, Rep. of Macedonia, 2006.

BGD
12, 12975–13039, 2015

Trajanovska, S., Blaženčić, J., Trajanovski, S., and Budzakoska-Gjoreska, B.: Distribution, morphological variability, ecology and the present state of *Nitella* from Lake Ohrid and its surroundings, Arch. Biol. Sci., 64, 549–556, doi:10.2298/ABS1202549T, 2012.

van Bergen, P. F., Nott, C. J., Bull, I. D., Poulton, P. R., and Evershed, R. P.: Organic geochemical studies of soils from the Rothamsted Classical Experiments – IV. Preliminary results from a study of the effect of soil pH on organic matter decay, Org. Geochem., 29, 1779–1795, 1998.

van der Meer, M. T. J., Schouten, S., van Dongen, B. E., Rijpstra, W. I. C., Fuchs, G., Sinninghe Damsté, J. S., de Leeuw, J. W., and Ward, D. M.: Biosynthetic controls on the ^{13}C contents of organic components in the photoautotrophic bacterium *Chloroflexus aurantiacus*, J. Biol. Chem., 276, 10971–10976, 2001.

Vogel, H., Wagner, B., Zanchetta, G., Sulpizio, R., and Rosén, P.: A paleoclimate record with tephrochronological age control for the last glacial–interglacial cycle from Lake Ohrid, Albania and Macedonia, J. Paleolimnol., 44, 295–310, 2010.

Volkman, J. K., Barrett, S. M., Dunstan, G. A., and Jeffrey, S. W.: C_{30}–C_{32} alkyl diols and unsaturated alcohols in microalgae of the class Eustigmatophyceae, Org. Geochem., 18, 131–138, 1992.

Volkman, J. K., Barrett, S. M., and Blackburn, S. I.: Eustigmatophyte microalgae are potential sources of C_{29} sterols, C_{22}–C_{28} *n*-alcohols and C_{28}–C_{32} *n*-alkyl diols in freshwater environments, Org. Geochem., 30, 307–318, 1999.

Wagner, B., Lotter, A. F., Nowaczyk, N., Reed, J. M., Schwalb, A., Sulpizio, R., Valsecchi, V., Wessels, M., and Zanchetta, G.: A 40 000-year record of environmental change from ancient Lake Ohrid (Albania and Macedonia), J. Paleolimnol., 41, 407–430, 2008.

Wagner, B., Wilke, T., Krastel, S., Zanchetta, G., Sulpizio, R., Reicherter, K., Leng, M., Grazhdani, A., Trajanovski, S., Levkov, Z., Reed, J., and Wonik, T.: More than one million years of history in Lake Ohrid cores, EOS T. Am. Geophys. Un., 95, 25–26, 2014.

Wang, F., Han, S., Hu, S., Xue, Y., Wang, J., Xu, H., Chen, L., Zhang, G., and Zhang, Y.: Two new secondary metabolites from *Xylaria* sp. cfcc 87468, Molecules, 19, 1250–1257, 2014.

Xu, Y., Mead, R. N., and Jaffé, R.: A molecular marker-based assessment of sedimentary organic matter sources and distributions in Florida Bay, Hydrobiologia, 569, 179–192, 2006.

Yamamuro, M. and Kayanne, H.: Rapid direct determination of organic-carbon and nitrogen in carbonate-bearing sediments with a yanaco mt-5 chn analyzer, Limnol. Oceanogr., 40, 1001–1005, 1995.

BGD
12, 12975–13039, 2015

Yang H, Ding, W. H., and Xie, S. C.: Distribution of microbial fatty acids and fatty alcohols in soils from an altitude transect of Mt. Jianfengling in Hainan, China: implication for paleoaltimetry and paleotemperature reconstruction, Sci. China Ser. D, 57, 999–1012, 2014.

Yunker, M. B., Belicka, L. L., Harvey, H. R., and Macdonald, R. W.: Tracing the inputs and fate of marine and terrigenous organic matter in Arctic Ocean sediments: a multivariate analysis of lipid biomarkers, Deep-Sea Res. Pt. II, 53, 3478–3508, 2005.

Zhang, Z., Zhao, M., Eglinton, G., Lu, H., and Huang, C.-Y.: Leaf wax lipids as paleovegetational and paleoenvironmental proxies for the Chinese Loess Plateau over the last 170 kyr, Quaternary Sci. Rev., 25, 575–594, 2006.

BGD
12, 12975–13039, 2015

Table 1. (a) Total organic carbon contents (TOC), organic carbon to total nitrogen ratio (TOC/TN) and carbonate ($CaCO_3$) contents of soils and leaf litter in the southeastern Ohrid Basin (TS = topsoil, TS/F = topsoil with white rot, S = soil, LL = leaf litter). For leaf litter, total nitrogen equals organic nitrogen. **(b)** Total organic carbon contents (TOC), organic carbon to organic nitrogen ratios (TOC/N_{org}) and carbonate contents ($CaCO_3$) of major Lake Ohrid macrophytes. Reed leaves (RL) were sampled near the Albanian–Macedonian border post (DG = Dogana). Submerged macrophytes were collected off Tushemisht (TU) and Pogradec (PG).

(a)

sample ID	location; coordinates	soil type; vegetation	TOC (%)	TOC/TN (atomic)	$CaCO_3$ (%)
SN-TS	above St. Naum springs;	Leptosol/Rendzina;	**11.0** ± 0.8	**17.5** ± 0.1	**7.7** ± 3.0
SN-LL	40°54′43.78″ N 20°44′35.18″ E, 708 m.a.s.l.	small oak, beech, shrubs	**41.1** ± 0.6	**28.8** ± 0.4	–
TP-TS	near Trpejca;	Leptosol/Rendzina;	**7.5** ± 0.2	**17.3** ± 0.0	**5.4** ± 0.8
TP-LL	40°58′45.46″ N 20°47′46.62″ E, 808 m.a.s.l.	small oak, beech, shrubs	**44.2** ± 0.3	**25.5** ± 0.2	–
TP-TS/F		with white rot	**10.1** ± 0.7	**17.4** ± 0.3	**5.4** ± 4.9
GN-TS	Galicica National Park;	Leptosol/Rendzina;	**8.9** ± 0.3	**15.3** ± 0.8	**7.4** ± 1.6
GN-LL	40°57′59.64″ N 20°48′52.10″ E, 1380 m.a.s.l.	mature beech forest	n.d	n.d.	–
DG-S	near border (dogana); 40°54′29.47″ N 20°43′48.04″ E, 708 m.a.s.l.	Chromic Luvisol/Terra Rossa (B-horizon); shrubs	**1.0** ± 0.1	**11.4** ± 0.8	**< 0.5**

BGD
12, 12975–13039, 2015

Table 1. Continued.

(b)					
sample ID	species	water depth (m)	TOC (%)	TOC/N_{org} (atomic)	$CaCO_3$ (%)
DG-RL	*Phragmites* leaves	0.5	44.2	13.3	–
TU-3	*Cladophora*	3	40.3	13.8	–
TU-4	*Potamogeton perfoliatus*	4	41.0	14.7	–
TU-6	*Potamogeton perfoliatus*	6	40.7	12.3	–
TU-12	*Chara tomentosa*	12	9.9	18.7	61.5
PG-14-II	*Chara gymnophyla*	14	10.4	17.0	71.2

BGD
12, 12975–13039, 2015

Table 2. Composition of the total lipid extracts (TLEs) and amounts of compound classes, sub-categories and individual lipids of soils, sediments, leaf litter, macrophytes and water filtrates from the Lake Ohrid Basin. Values are given as percentages of the total lipids ($\%_{lipids}$); SN = St Naum, TP = Trpejca, GN = Galicica National Park, DG = Dogana; ll = leaf litter, ts = topsoil, ms = mineral soil, hc = high-carbonate sediment, lc = low-carbonate sediment, clad. = *Cladophora*, potam. = *Potamogeton*, chara. = *Characeae* spp., phrag-r, -s, -l = *Phragmites* spp. roots, stem, leaves. Bold script indicates the dominant compound class in each category.

site	SN	TP	GN	SN	TP	TP/F	GN	DG	Lz1120		TU/PG	PG	TU/PG	DG	DG	DG	Co/DEEP
sample type/species	ll	ll	ll	ts	ts	ts	ts	ms	hc	lc	clad.	potam.	chara.	phrag-r	phrag-s	phrag-l	filtrates*
number of samples	2	1	1	2	2	2	2	1	8	3	2	2	3	1	1	2	4
total lipids ($\mu g\,g^{-1}$ dry weight)	643	471	653	63	97	89	79	1.3	40	13	1068	224	533	443	345	1723	–
lipid fractions (%)																	
n-alkanoic acids (FA)	**35.0**	**38.3**	22.5	**34.9**	**35.9**	**39.6**	**29.0**	14.7	**39.6**	19.6	**44.8**	22.7	32.7	31.8	**35.8**	15.0	**33.1**
hydroxy acids (OH-FA)	3.9	2.1	0.9	5.6	7.9	5.3	5.4	1.4	4.6	3.3	0.2	0.3	–	3.5	1.4	0.3	1.3
branched alkanoic acids	0.2	–	0.1	2.6	1.5	1.4	1.5	0.6	0.9	1.2	0.6	0.04	1.7	0.4	0.1	–	1.9
mono-unsaturated alkenoic acids	6.9	7.5	20.6	19.4	22.1	17.1	25.4	14.7	0.2	0.2	40.6	6.0	20.7	4.7	15.5	1.9	29.9
poly-unsaturated alkenoic acids	9.8	8.2	17.3	3.4	5.4	5.6	5.4	5.4	–	–	9.5	**35.3**	**36.1**	**43.6**	34.6	**57.5**	7.6
n-alcohols (OH)	3.2	3.1	6.3	15.3	13.6	15.8	16.6	**47.6**	21.1	**37.0**	0.8	1.5	0.1	0.6	1.4	19.3	4.1
n-alkanes	4.8	6.7	5.4	3.4	2.2	1.7	3.1	3.5	1.5	3.3	0.05	1.0	–	–	–	0.3	n.a.*
methyl ketones	0.04	–	–	–	–	–	–	–	0.4	0.9	–	–	–	–	–	–	–
sterols	13.1	15.7	**23.7**	13.2	9.7	11.0	12.8	11.0	14.7	24.2	3.6	32.9	8.7	12.3	10.6	4.9	20.5
others	23.1	18.5	3.2	2.1	1.7	2.5	0.9	1.2	17.0	16.6	–	0.3	0.1	3.2	0.7	0.8	1.6
***n* -alkanoic acids**																	
$\Sigma\ C_{14}$–C_{19} FA (short-chain)	**15.5**	**17.1**	**13.8**	10.5	9.9	13.2	6.1	**7.1**	7.3	7.2	**44.3**	**19.2**	**31.7**	**19.4**	**28.1**	**12.7**	**26.7**
$\Sigma\ C_{20}$–C_{25} FA (mid-chain)	6.4	10.0	5.7	11.3	**13.3**	11.4	9.5	5.7	13.7	7.3	0.5	2.8	1.0	10.0	5.6	1.0	5.4
$\Sigma\ C_{26}$–C_{34} FA (long-chain)	13.2	11.2	2.9	**13.1**	12.7	**15.0**	**13.4**	1.8	**18.6**	5.1	0.1	0.8	0.01	2.3	2.0	1.3	1.1
hydroxy acids																	
$\Sigma\omega$-hydroxy acids	0.3	0.1	**0.6**	**4.4**	**6.1**	**4.0**	**4.7**	**1.1**	**4.4**	**2.6**	–	0.02	–	1.6	0.4	–	0.6
$\Sigma\alpha$-hydroxy acids	**3.5**	**2.0**	0.2	1.2	1.7	1.3	0.7	0.3	0.3	0.7	**0.2**	**0.3**	–	**2.0**	**1.0**	**0.3**	**0.7**
branched alkanoic acids																	
C_{14}–C_{16} branched FA	**0.2**	–	**0.1**	**1.7**	**0.8**	**0.9**	**1.0**	0.6	**0.9**	**1.1**	**0.4**	–	0.7	–	0.1	–	0.6
C_{17}–C_{19} branched FA	–	–	–	0.9	0.7	0.5	0.5	–	0.01	0.1	0.1	–	**1.0**	**0.4**	–	–	**1.1**
C_{20}–C_{25} branched FA	–	–	–	–	–	–	–	–	0.01	–	–	–	–	–	–	–	0.2
mono-unsaturated alkenoic acids																	
$C_{16:1}$ FA	0.7	0.9	1.0	4.4	5.2	8.4	2.7	4.0	–	–	**29.3**	2.7	**11.8**	–	**13.1**	**1.7**	4.9
$C_{18:1}$ FA	**6.1**	**6.3**	**19.4**	**14.5**	**16.6**	**8.5**	**22.5**	**10.2**	**0.2**	**0.5**	11.3	**2.7**	7.1	0.5	0.7	0.2	**21.0**
$C_{19:1}$–$C_{24:1}$ FA	0.1	0.3	0.2	0.5	0.2	0.2	0.2	0.5	–	–	0.02	0.6	1.8	**4.1**	1.2	0.03	1.95
poly-unsaturated alkenoic acids																	
$C_{18:2}$ FA	**7.9**	**8.2**	**17.3**	**3.4**	**5.4**	**5.3**	**5.4**	**5.4**	–	–	2.5	11.2	8.8	**27.0**	**21.1**	10.0	**7.4**
$C_{18:3}$ FA	**2.0**	–	–	**0.02**	**0.1**	**0.3**	**0.02**	–	–	–	**3.7**	**22.9**	**11.3**	16.4	12.7	**47.6**	–
	TERRESTRIAL								SEDIM.					AQUATIC			

BGD
12, 12975–13039, 2015

Table 2. Continued.

site	SN	TP	GN	SN	TP	TP/F	GN	DG	Lz1120		TU/PG	PG	TU/PG	DG	DG	DG	Co/DEEP
sample type/species	II	II	II	ts	ts	ts	ts	ms	hc	lc	clad.	potam.	chara.	phrag-r	phrag-s	phrag-l	filtrates*
poly-unsaturated alkenoic acids																	
$C_{20:5}$ FA (EPA)	–	–	–	–	–	0.1	–	–	–	–	1.5	0.6	5.5	–	0.7	–	0.2
$C_{22:6}$ FA (DHA)	–	–	–	–	–	–	–	–	–	–	0.1	0.2	2.2	–	–	–	–
***n*-alcohols**																	
Σ C_{12}–C_{19} OH (short-chain)	0.2	0.1	1.4	0.8	0.7	0.5	0.6	0.6	1.1	1.3	0.2	0.1	**0.1**	0.1	–	0.1	1.7
Σ C_{20}–C_{25} OH (mid-chain)	**1.9**	**1.5**	**3.8**	**7.5**	**6.8**	6.3	5.3	16.6	7.6	11.1	0.1	**0.8**	0.01	**0.3**	0.4	0.3	**2.2**
Σ C_{26}–C_{34} OH (long-chain)	1.1	1.4	1.1	7.0	6.1	**9.0**	**10.7**	**30.4**	**12.4**	**18.1**	**0.4**	0.6	–	0.2	**1.1**	**18.8**	0.2
***n*-alkanes**																	
Σ C_{19}–C_{20} (short-chain)	–	–	–	–	–	–	–	–	–	0.02	–	–	–	–	–	–	n.a. = not available
Σ C_{21}–C_{26} (mid-chain)	0.5	0.3	0.3	0.2	0.1	0.1	0.1	0.3	0.2	0.4	–	**0.4**	–	–	–	**0.06**	n.a.*
Σ C_{27}–C_{33} (long-chain)	**4.3**	**6.4**	**5.1**	**3.2**	**2.1**	**1.6**	**2.9**	**3.2**	**1.3**	**3.0**	**0.05**	0.3	–	–	**0.3**	–	n.a.*
sterols																	
cholesterol	–	0.1	–	0.5	0.5	0.2	0.9	0.6	1.5	1.9	0.6	0.4	2.3	0.1	–	0.4	**8.3**
cholestanol	–	–	–	–	–	–	–	–	0.8	2.2	–	–	–	–	–	–	–
ergosterol	0.2	–	0.4	0.1	0.2	0.1	0.1	–	–	–	–	–	–	–	–	–	–
stigmasterol	0.03	0.2	0.3	0.4	0.6	0.6	0.3	–	0.3	0.5	–	8.1	0.1	1.6	1.7	0.6	0.7
sitosterol	**10.5**	**11.0**	**16.6**	**9.5**	**5.9**	**7.8**	**9.4**	**9.1**	1.7	3.0	**2.8**	**15.3**	**3.4**	**10.3**	**8.6**	**3.6**	5.6
stigmastanol	0.3	0.6	0.4	0.7	0.5	0.5	0.8	0.9	3.3	**6.2**	–	–	–	0.3	0.3	–	–
dinosterol	–	–	–	–	–	–	–	–	1.2	1.1	–	–	–	–	–	–	–
dinostanol	–	–	–	–	–	–	–	–	1.4	1.8	–	–	–	–	–	–	–
β-sitostenone	1.6	2.9	5.1	1.0	0.9	0.6	0.8	0.3	–	–	–	–	–	–	–	–	–
lanosterol	–	–	–	–	–	–	–	–	**3.3**	5.9	–	–	–	–	–	–	–
others																	
dicarboxylic acids (DiFA)	0.2	–	–	**1.0**	0.5	**1.0**	**0.4**	–	–	–	–	–	–	**0.2**	–	–	–
α-tocopherol	**2.6**	**3.6**	**3.2**	0.7	0.4	0.3	0.3	–	0.7	0.4	–	**0.2**	**0.1**	0.1	0.1	**0.8**	–
$\alpha + \beta$-amyrin	1.2	1.8	–	0.7	**0.8**	0.7	0.1	**1.2**	0.7	1.2	–	–	–	–	–	–	–
tetrahymanol	–	–	–	–	–	–	–	–	0.7	1.5	–	–	–	–	–	–	–
1,15(ω16)C_{30} diol	–	–	–	–	–	–	–	–	2.0	2.6	–	–	–	–	–	–	–
1,15(ω16)C_{30} keto-ol	–	–	–	–	–	–	–	–	1.0	1.3	–	–	–	–	–	–	–
1,15(ω18)C_{32} diol	–	–	–	–	–	–	–	–	0.8	0.8	–	–	–	–	–	–	–
17β(H),21β(H)-bishomohopanoic acid	–	–	–	–	–	–	–	–	**9.3**	**6.1**	–	–	–	–	–	–	–
	TERRESTRIAL								SEDIM.				AQUATIC				

* Indicates only polar fractions were analysed. For the full list of compounds see "Supplement".

BGD
12, 12975–13039, 2015

Table A1. Abbreviations used for lipid biomarkers and their IUPAC names.

***n*-Alkanes**	
These are abbreviated by their carbon number, for example:	
n-C_{27}	*n*-heptadocosane
Fatty acids	
n-Alkanoic acids are abbreviated by their carbon number, for example:	
C_{16} FA	hexadecanoic acid
C_{18} FA	octadecanoic acid
Monounsaturated fatty acids (MUFAs) are abbreviated using IUPAC recommended numerical symbols, for example:	
$C_{16:1}$ (*cis*-9)	*cis*-9-hexadecenoic acid
$C_{18:1}$ (*cis*-9)	*cis*-9-octadecenoic acid
$C_{20:1}$ (*cis*-9)	*cis*-9-docasenoic acid
Polyunsaturated acids (PUFAs) are abbreviated in the same way, but where double bond positions are unsure, no designated position is given, for example:	
$C_{18:2}$	octadecanadienoic acid
Branched fatty acids are abbreviated as follows:	
iso-C_{15}	13-methyltetradecanoic acid
anteiso-C_{15}	12-methyltetradecanoic acid
iso-C_{16}	14-methylpentadecanoic acid
iso-C_{17}	15-methylhexadecanoic acid
anteiso-C_{17}	14-methylhexadecanoic acid
Hydroxy fatty acids, either $\alpha-$ or $\omega-$ are abbreviated as follows:	
C_{22} α–OH-FA	2-hydroxydocosanoic acid
C_{22} ω–OH-FA	22-hydroxydocosanoic acid
Diacids are denoted α,ω-DiFAs, for example:	
C_{16} α,ω-DiFA	hexadecadioic acid

BGD
12, 12975–13039, 2015

Table A1. Continued.

Fatty alcohols	
n-Alcohols are abbreviated by their carbon number, for example:	
C_{16} OH	1-hexadecanol
C_{18} OH	1-octadecanol
Branched alcohols are abbreviated as follows:	
iso-C_{15} OH	13-methyltetradecan-1-ol
anteiso-C_{15} OH	12-methyltetradecan-1-ol
Long chain diols are abbreviated as follows:	
C_{30} 1,15-diol	1,15-triacontadiol
C_{32} 1,15-diol	1,15-dotriacontadiol
Long-chain ketones	
Long-chain hydroxy-ketones are abbreviated as follows:	
1,15(ω16)C_{30}keto-ol	1-hydroxy-tetradecan-15-one
Terpenes	
Isoprenoids	
α-tocopherol	2,5,7,8-Tetramethyl-2-(4,8,12-trimethyltridecyl)-6-chromanol
Sterols	
β-sitosterol	24β-ethylcholest-5-en-3β-ol
β-sitostenone	24β-ethylcholest-4-en-3β-one
stigmasterol	24β-ethylcholesta-5,22*E*-dien-3β-ol
stigmastanol	24-ethyl-5α(H)-cholestan-3β-ol
cholesterol	cholest-5-en-3β-ol
cholestanol	5α(H)-cholestan-3β-ol
coprostanol	5β(H)-cholestan-3α-ol
epicoprostanol	5β(H)-cholestan-3β-ol
epicholestanol	5α(H)-cholestan-3α-ol
brassicasterol	24β-methylcholesta-5,22*E*-dien-3β-ol
campesterol	24β-methylcholest-5-en-3β-ol
ergosterol	ergosta-5,7,22-trien-3β-ol
dinosterol	4α,23,24-trimethylcholest-22*E*-dien-3β-ol
dinostanol	4α,23,24-trimethylcholestan-3β-ol
lanosterol	5α-lanosta-8,24-en-3β-ol
Triterpenoids	
taraxasterol	5α-taraxast-20(30)-en-3β-ol
tetrahymanol	gammaceran-3β-ol
β-amyrin	olean-12-en-3β-ol

BGD
12, 12975–13039, 2015

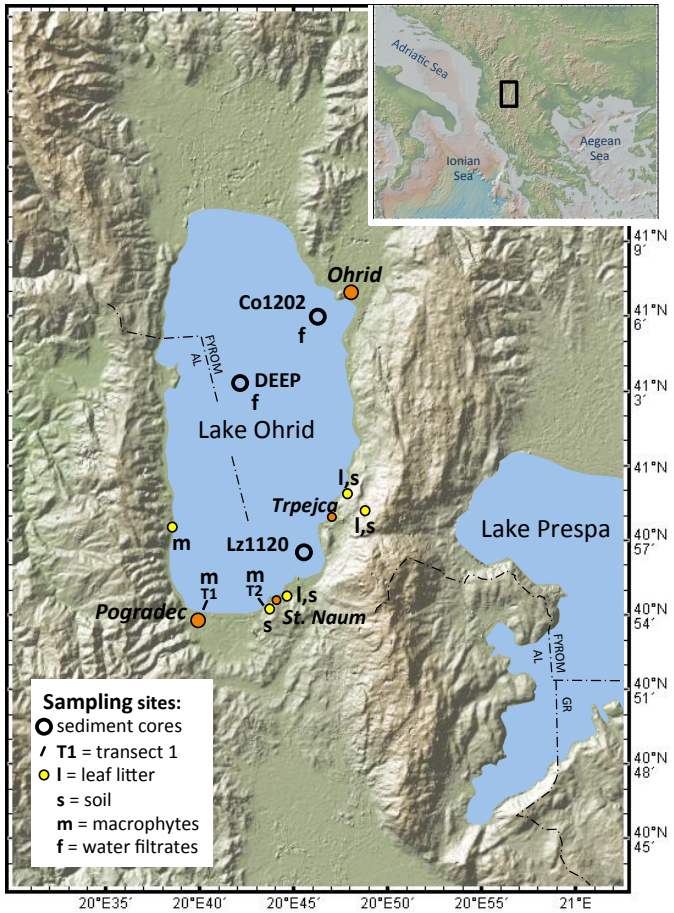

Figure 1. Locations of sediment core Lz1120 and sampling sites for modern materials in the Ohrid Basin. Lake Prespa contributes 28 % of the inflow of meteoric water through karst systems. Inset: location of Lake Ohrid in the Balkans region of South Eastern Europe.

BGD
12, 12975–13039, 2015

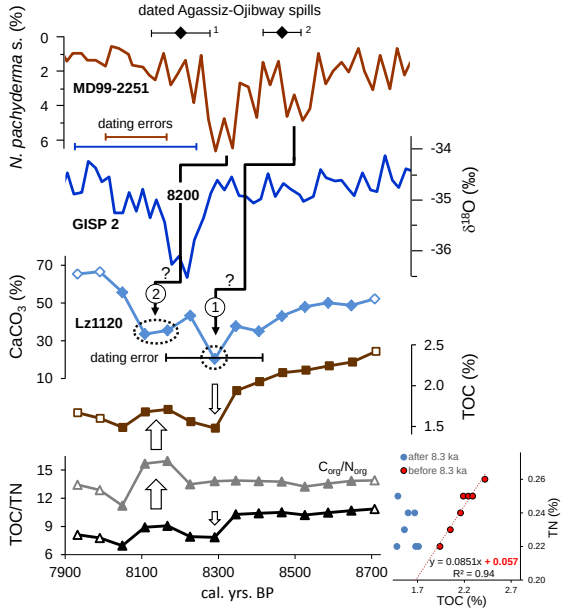

Figure 2. Records of carbonate ($CaCO_3$), total organic carbon (TOC) and the organic carbon to total nitrogen ratio (TOC/TN) of core Lz1120 compared to proxy data from the North Atlantic. Phases of increased percentages of *N. pachyderma* s. in MD99-2251 indicate at least two southward shifts of colder surface waters (Ellison et al., 2006) while the excursion in the $\delta^{18}O$ record of Greenland ice cores (GISP), which first defined the 8.2 ka event, indicates a drop in atmospheric temperature over the Greenland Ice Sheet (Grootes et al., 1993). The dashed circles mark those samples that are discussed as low-carbonate samples in carbonate minima 1 and 2 and are possibly corresponding to the climatic deteriorations occurring over the course of the 8.2 ka event caused by at least two catastrophic freshwater spills into the North Atlantic ([1] Roy et al., 2011; [2] Lajeunesse and St-Onge, 2008). White arrows highlight different fluxes of organic carbon and total nitrogen during the carbonate minima. Insert: TOC vs. TN for samples from before (red) and after (blue) 8.3 ka.

BGD
12, 12975–13039, 2015

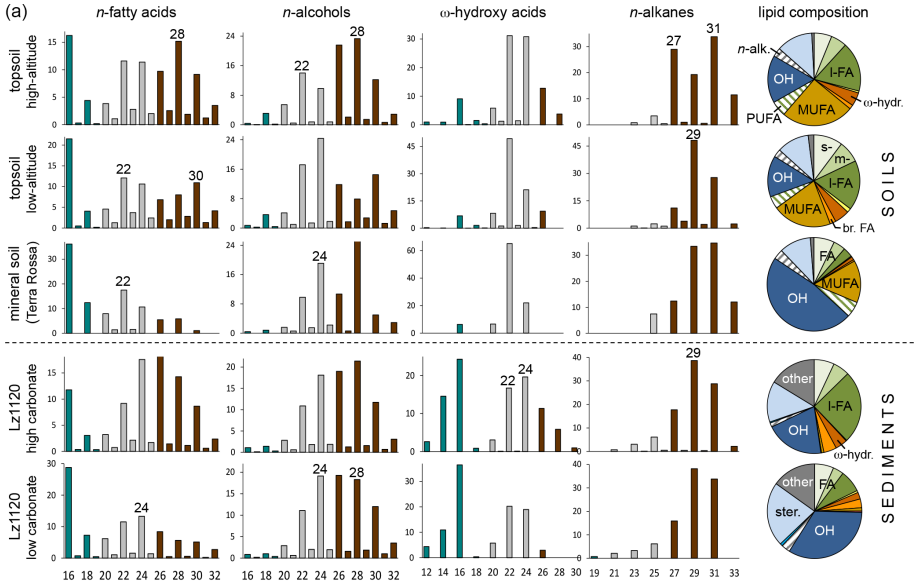

Figure 3a. Chain-length distributions of *n*-alkyl compounds (bar diagrams) in high- and low-altitude topsoil, mineral soil and early Holocene sediments and the composition of GC-amendable lipids (pie diagrams). Chain-length distribution *y* axis values are percentages of the total amount of each compound class, i.e. $\%_{FA}$, $\%_{OH}$ etc.; s-, m-, l-FA = short-, mid- and long-chain FA; MUFA = mono-unsaturated FA; PUFA = poly-unsaturated FA; ster. = sterols; hydr. = hydroxy acids; br. FA = branched FA. Note the distinct shift towards C_{22} and C_{24} in chain-length distributions of FAs and towards C_{24} in chain-length distributions of OHs from high to low carbonate sediment samples. C_{12} and C_{14} ω-hydroxy acids in the sediments appear to derive from an in situ source.

BGD
12, 12975–13039, 2015

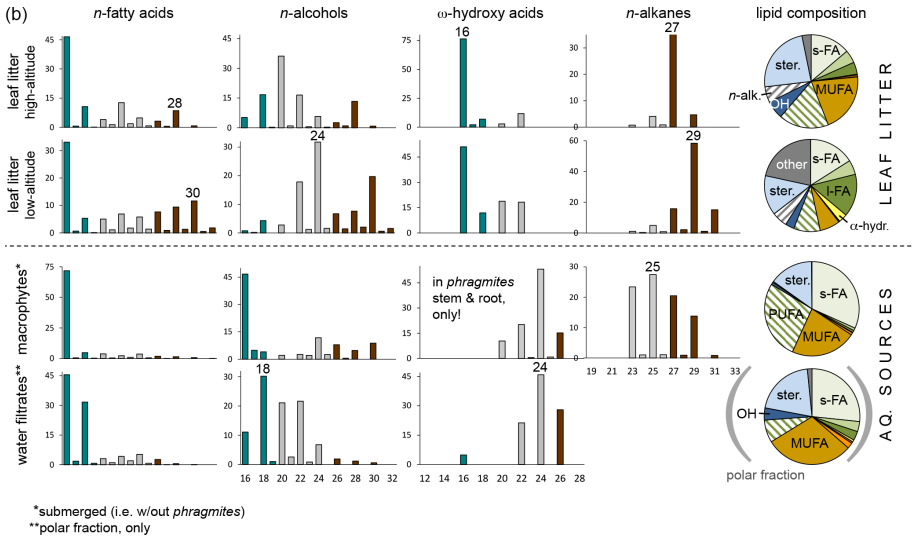

Figure 3b. Chain-length distributions of *n*-alkyl compounds (bar diagrams) in high- and low-altitude leaf litter, macrophytes and water filtrates and the composition of GC-amendable lipids (pie diagrams); labelling as in Fig. 3a. Macrophyte data derives from submerged species, except for the *ω*-hydroxy acids, which exclusively occur in (emergent) *Phragmites* sp. Water filtrate data does not include non-polar *n*-alkanes as these were separated from the polar TLE fractions prior to further sample processing.

BGD
12, 12975–13039, 2015

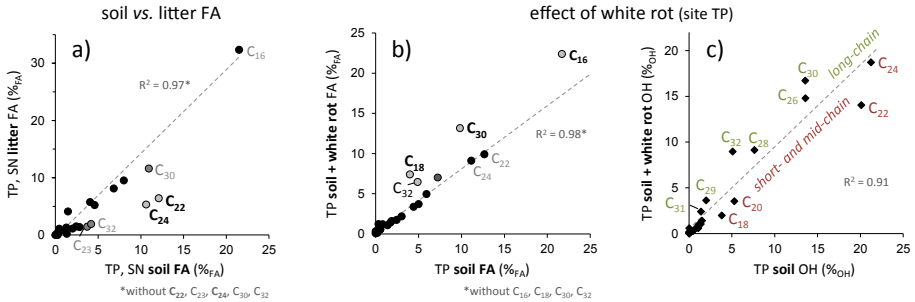

Figure 4. Correlations of compound class-specific relative abundances of **(a)** *n*-alkanoic acids in soils and leaf litter of the low-altitude, oak-dominated sites (TP, SN), **(b)** *n*-alkanoic acids and **(c)** *n*-alcohols in the two soil samples from site TP, one of which is affected by white rot. The patterns illustrate enrichment of mid-chain FA ($C_{22,24}$) from leaf litter to soil and of long-chain *n*-alcohols ($C_{26–32}$) as well as long-chain FA ($C_{30,32}$) and short-chain FA ($C_{16,18}$) due to visibly enhanced fungal degradation (white rot) within the soil at site TP. Chain-length shifts in the latter suggest either selective degradation or biosynthesis of specific compounds by fungi.

BGD
12, 12975–13039, 2015

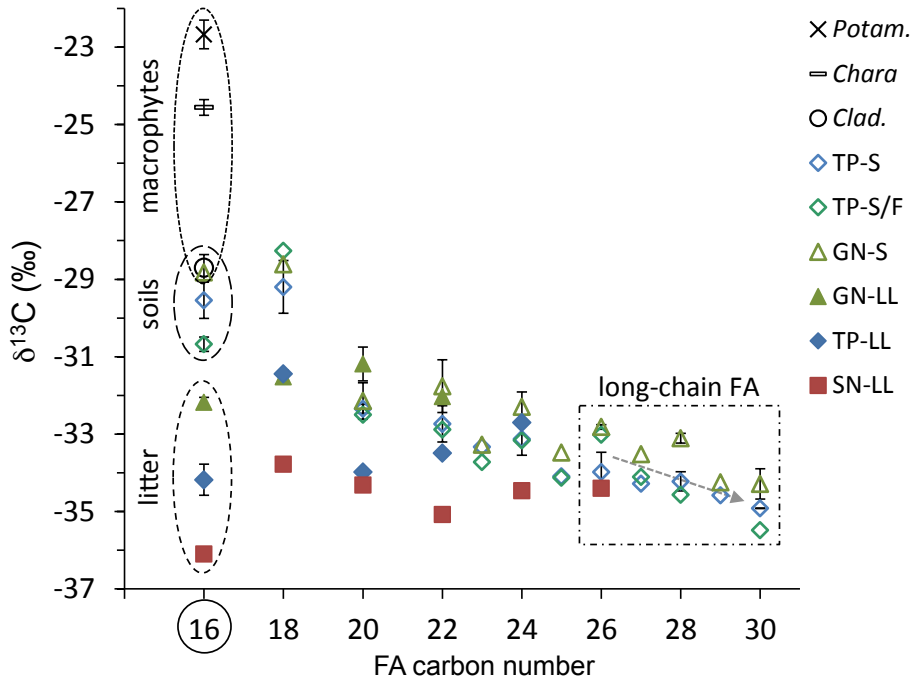

Figure 5. Carbon-isotope composition ($\delta^{13}C$) of *n*-alkanoic acids from macrophytes, leaf litter and topsoils (LL = leaf litter, S = soil, S/F = soil visibly affected by fungi). While the $\delta^{13}C$ values for C_{16} FA are heaviest in macrophytes and lightest in leaf litter, as expected for aquatic and terrestrial biomass, there is a significant shift toward heavier values for C_{16} FA in soils that even overlap with the value for *Characeae* spp. Also note the trend of decreasing $\delta^{13}C$ values of long-chain FAs (dashed arrow) and the lower values of odd-numbered long-chain FAs.

BGD
12, 12975–13039, 2015

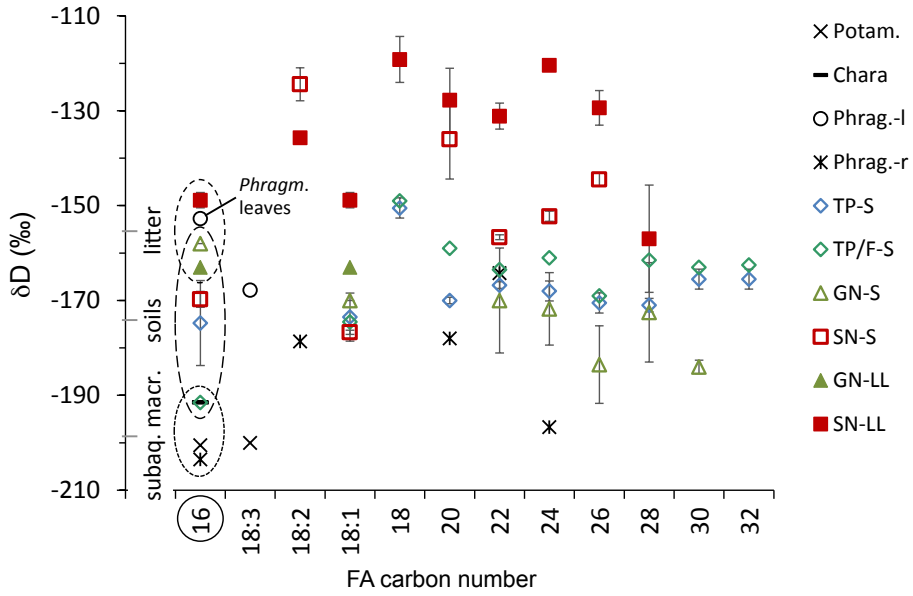

Figure 6. Hydrogen-isotope composition (δ^2H) of *n*-alkanoic acids from macrophytes, leaf litter and topsoils (LL = leaf litter, S = soil, S/F = soil visibly affected by fungi, l = leaves, r = roots). Submerged macrophytes (*Potamogeton* spp., *Chara* spp.) show the lightest values, as expected. Leaves of *Phragmites* spp. plot within the range covered by litter from sites SN and GN. δ^2H values of C_{16} FA from soil and litter overlap, while the sample affected by white rot plots in the range of submerged macrophytes. Note the significantly higher δ^2H values of FAs from site SN that probably result from the intake of water vapor from the St. Naum karst springs, which is enriched in deuterium compared to the local meteoric water line (Matzinger et al., 2006).

BGD
12, 12975–13039, 2015

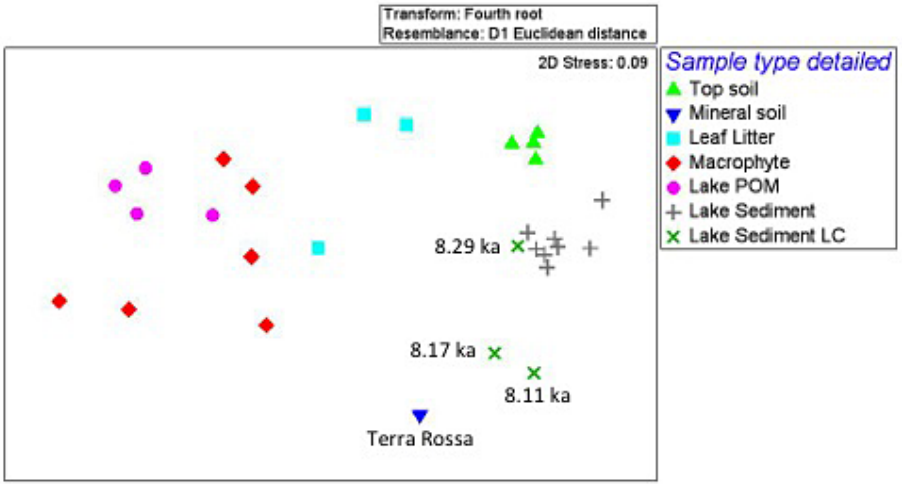

Figure 7. MDS plot showing separation of sample types in Euclidean space. For details see methodology Sect. 2.4. Lake Sediment LC in the key denotes the three sediment samples with low carbonate contents (samples from 8.11, 8.17 and 8.29 ka; see Fig. 8).

BGD
12, 12975–13039, 2015

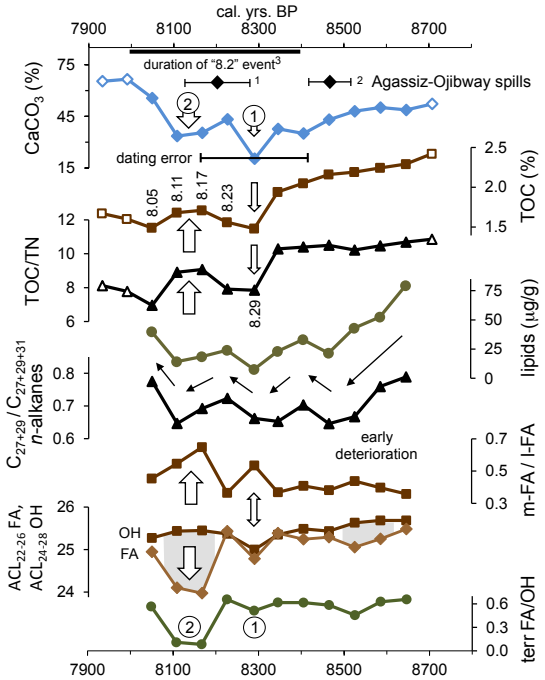

Figure 8. Records from elemental ($CaCO_3$, TOC, TOC/TN) and lipid biomarker analyses of sediment core Lz1120 over the course of the 8.2 ka climate deterioration. White arrows indicate contrasting response of elemental and biomarker proxies in response to the reduced carbonate supply, i.e. in carbonate minima. Black diamonds indicate Agassiz–Ojibway freshwater spillages dated by [1] Roy et al. (2011) and [2] Lajeunesse and St-Onge (2008), [3] duration of 8.2 climate deterioration (Barber et al., 1999). While *n*-alkane composition (C_{27} and C_{29} relative to C_{31}) appears to co-vary with the total concentration of lipids in the sediment (indicated by the black arrows), proxies based on *n*-alkanoic acid and *n*-alcohol distribution appear to correspond to the environmental changes indicated by the variable supply of carbonate and non-carbonate material.

BGD
12, 12975–13039, 2015